A multi-phase transitioning peptide hydrogel for suturing ultra-small vessels

Daniel J. Smith, Gabriel A. Brat, Scott H. Medina, Dedi Tong, Yong Huang, Johanna Grahammer, Georg J. Furtmüller, Byoung Chol Oh, Katelyn J. Nagy-Smith, Piotr Walczak, Gerald Brandacher, and Joel P. Schneider.

Supplemental Information Table of Contents

Content

Abbreviations: Acetic acid (AcOH), acetic anhydride (Ac_2O), 1,3-bis(tris(hydroxymethyl)methylamino)propane (BTP), di-*tert*-butyl dicarbonate (Boc_2O), diisopropylethylamine (DIEA), 4-dimethylamino pyridine (DMAP), dimethylformamide (DMF), dimethylsulfoxide (DMSO), ethyl acetate (EtOAc), N-(9-Fluorenylmethoxycarbonyloxy)succinimide (Fmoc-OSu), acetonitrile (MeCN), methanol (MeOH), *N*-methyl-2-pyrrolidinone (NMP), trifluoroacetic acid (TFA), tetrahydrofuran (THF), triisopropylsilane (TIPS).

Materials and General Methods. All reagents and solvents were used as received. All Fmoc-protected amino acids were purchased from Novabiochem. PL-rink amide resin was purchased from Polymer Laboratories. 1-H-benzotriazolium-1-[*bis*(dimethylamino) methylene]-5-chloro-hexafluorophosphate-(1-),3-oxide (HCTU) was obtained from Peptides International. Trifluoroacetic acid and triisopropylsilane were obtained from Acros Organics. Diethyl ether was purchased from Fisher Scientific. Unless otherwise stated, all other reagents were purchased from Sigma Aldrich. ^{1}H and ^{13}C NMR chemical shifts were recorded on a Varian spectrometer and are reported in ppm and were assigned based on ^{1}H-^{1}H COSY and ^{1}H-^{13}C HMQC experiments. Nominal mass spectra for small molecules were obtained using electrospray ionization (ESI). Liquid chromatography mass spectroscopy of peptides was performed using a linear gradient of 0-90% MeCN containing 0.1% TFA in water containing 0.1% TFA over 40 minutes on C18 stationary phase coupled with an electrospray ionization (ESI) detector. Molecular models for Figure 2b were prepared in Discovery Studio 4.0 (Accelrys/BioVia). Peptides were pre-organized in a canonical β-hairpin conformation containing a type II' β-turn. Eight hairpins were manually docked to form a bilayer, each layer consisting of four peptides. Assemblies were energy minimized employing a CHARMm forcefield and implicit generalized Borne water. A two-step protocol was employed for the minimization. First, all backbone atoms were constrained and the side chain atoms minimized using a steepest decent algorithm. This was followed by an all atom minimization using steepest decent with an RMS gradient tolerance of 3, followed by a conjugate gradient algorithm. All animal studies were performed using male C57BL/6 mice at 8 – 10 weeks of age.

Peptide Synthesis and Purification: Peptides were synthesized on PL-Rink amide resin using an automated ABI 433A peptide synthesizer (Applied Biosystems, CA) and a Tribute peptide synthesizer (Protein Technologies, Inc., AZ). Synthesis was carried out via solid-phase Fmoc-based chemistry with HCTU activation. Fmoc-*L*-Glu(MNI)-OH was incorporated into peptides by reacting the peptide on resin with a solution of 3 eqv. of amino acid, 2.7 eqv. of HCTU, and 6 eqv. of diisopropylethylamine in NMP (3.75 mL) for 30 mins. Dried resin-bound peptides were cleaved from the resin and side-chain deprotected by a trifluoroacetic acid: triisopropylsilane: deionized water (95:2.5:2.5) cocktail for 2 h under argon atmosphere. Crude peptides were precipitated using cold ethyl ether and then lyophilized. The resulting crude APC1 and APC2 peptides were purified by RP-HPLC (Vydac C18 Column) at 40 °C using an isocratic gradient from 0 – 2 minutes at 0% standard B, then utilizing a linear gradient from 0 – 20% standard B for 6 minutes followed by a gradient of 20 – 100% standard B over 160 minutes. Here, standard A is 0.1% TFA in water and standard B is 90% MeCN, 9.9% H_2O, and 0.1% TFA. Both peptides elute at 33 minutes. Control peptides cAPC1 and cAPC2 were also purified by RP-HPLC (Vydac C18 Column) at 40 °C using an isocratic gradient from 0 to 2 minutes at 0% standard B, then utilizing a linear gradient from 0 – 16% standard B for 4 minutes followed by a gradient of 16 – 100% standard B over 168 minutes. Both peptides elute at 28 minutes. Purified peptide solutions were lyophilized, resulting in pure peptide powders that were utilized in all assays. Purity of each peptide was confirmed by analytical HPLC and positive mode electrospray ionization - mass spectrometry. Fmoc-Glu(MNI)-OH (**7**) was prepared by a modified procedure as outlined below[1,2]. NMR spectra for **7** and the intermediates of its synthesis are also provided. Claycop was prepared in a 2:3 ratio of $Cu(NO_3)_2$ and montmorillonite K10 as described previously[3].

Synthesis of Fmoc-Glu(MNI)-OH

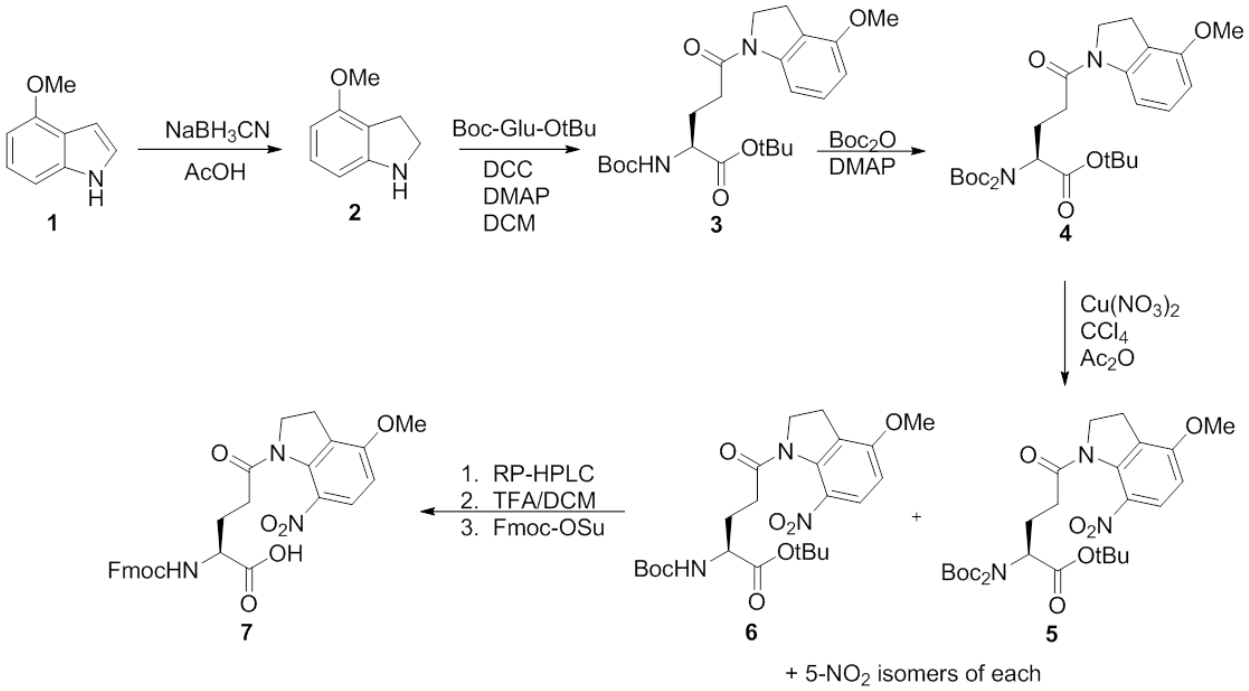

*4-Methoxyindoline (**2**).* Sodium cyanoborohydride (2.29 g, 36.5 mmol) was added portionwise over 20 minutes to a stirring solution of 4-methoxyindole (1.47 g, 10 mmol) in AcOH (30 mL). After the addition, the reaction was stirred for 30 minutes, water (30 mL) was added, and the solvent was removed in vacuo. The residue was neutralized by the addition of 1 M $NaHCO_3$ and extracted 2x50 mL with EtOAc. The combined organic extracts were washed with 0.5 M NaOH (30 mL), dried with $MgSO_4$, and concentrated in vacuo to yield 1.43 g of crude **2** (9.6 mmol, 96%) as an oil, which was used without any further purification. ^{1}H NMR (400 MHz, $CDCl_3$): δ = 7.00 (t, J = 8.0 Hz, 1H, Ar*H*-4), 6.33 (d, J = 7.8 Hz, 1H, Ar*H*-3), 6.30 (d, J = 8.2 Hz, 1H, Ar*H*-5), 3.82 (s, 3H, C*H*$_3$-9), 3.57 (t, 2H, C*H*$_2$-8), 2.99 (t, 2H, C*H*$_2$-7). ^{13}C NMR (101 MHz, $CDCl_3$): δ = 156.6 (6), 153.4 (2), 128.7 (4), 115.9 (1), 103.3 (3), 101.7 (5), 55.4 (9), 47.6 (8), 27.0 (7). ESI-MS calcd for $C_9H_{11}NO$ (MH^+) 150.1, found 150.1.

*4-Methoxyindolinyl N-α-(tert-butoxycarbonyl)-L-glutamic acid α-tert-butyl ester (**3**).* To a stirring solution of crude **2** (1.89 g, 12.7 mmol) in CH_2Cl_2 (98 mL) was added *N*-α-(*tert*-

butoxycarbonyl)-*L*-glutamic acid α-*tert*-butyl ester (5.0 g, 16.5 mmol), followed by *N*,*N*'-dicyclohexylcarbodiimide (3.40 g, 16.5 mmol) and DMAP (2.01 g, 16.5 mmol). The mixture was stirred at room temperature for 20 h, after which time the precipitated urea was filtered and washed with CH_2Cl_2. The filtrate was washed with 1 M $NaHCO_3$ (50 mL), 0.5 M HCl (100 mL), brine (50 mL), dried with $MgSO_4$, concentrated, and purified on silica gel using an automated flash chromatography system employing a gradient of ethyl acetate in hexanes; product elutes at ~40% ethyl acetate to yield 5.3 g of **3** (12.2 mmol, 96%) as a light yellow foam. $[\alpha]_D^{20} = +8.0^o$ (*c* 1.0, $CDCl_3$); ^{1}H NMR (400 MHz, $CDCl_3$): δ = 7.83 (d, J = 8.1 Hz, 1H, Ar*H*-16), 7.16 (t, J = 8.2 Hz, 1H, Ar*H*-17), 6.57 (d, J = 8.2 Hz, 1H, Ar*H*-18), 5.23 (d, 1H, N*H*-1), 4.27 – 4.16 (m, 1H, C*H*-2), 4.03 (t, 2H, CH_2-15), 3.83 (s, 3H, CH_3-20), 3.09 (t, 2H, CH_2-14), 2.59 – 2.39 (m, 2H, CH_2-10), 2.31 – 2.21 (m, 1H, C*H*H-9), 2.06 – 1.98 (m, 1H, CH*H*-9'), 1.47 (s, 9H, C(CH_3)$_3$-8), 1.42 (s, 9H, C(CH_3)$_3$-5). ^{13}C NMR (101 MHz, $CDCl_3$): δ = 171.7 (11), 170.3 (3), 155.8 (6), 155.7 (19), 144.4 (12), 129.1 (17), 118.4 (13), 110.2 (16), 106.1 (18), 82.2 (4), 79.8 (7), 55.4 (20), 53.9 (2), 48.5 (15), 32.4 (10), 28.4 (5), 28.1 (8), 27.9 (9), 25.2 (14). ESI-MS calcd for $C_{23}H_{34}N_2O_6$ (MH^+) 435.3, found 435.3.

*4-Methoxyindolinyl N-α-(di-tert-butoxycarbonyl)-L-glutamic acid α-tert-butyl ester (**4**).* To a solution of **3** (869 mg, 2 mmol) in CH_2Cl_2 (8 mL) and triethylamine (12 mL) was added Boc_2O (1.09 g, 5 mmol) and DMAP (29.3 mg, 0.24 mmol). The solution was heated at reflux for 5 h, after which additional Boc_2O (550 mg, 2.5 mmol) was added and the reaction was stirred overnight at room temperature. After removing the solvent in vacuo, the residue was dissolved in ethyl acetate (40 mL), washed with 1 M $KHSO_4$ (25 mL), 1M $NaHCO_3$ (25 mL), brine (25 mL), dried with $MgSO_4$, concentrated, and purified on silica gel using and automated flash chromatography system employing a gradient of ethyl acetate in hexanes; product elutes at ~30% ethyl acetate to yield 913 mg of **4** (1.7 mmol, 85%) as a light yellow foam. $[\alpha]_D^{20} = -32.0^o$ (*c* 1.0, $CDCl_3$); ^{1}H NMR (400 MHz, $CDCl_3$): δ = 7.86 (d, J = 8.1 Hz, 1H, Ar*H*-18), 7.15 (t, J = 8.2 Hz, 1H, Ar*H*-19), 6.56 (d, J = 8.1 Hz, 1H, Ar*H*-20), 4.87 (dd, 1H, C*H*-7), 4.05 (t, 2H, CH_2-

17), 3.83 (s, 3H, CH_3-22), 3.09 (t, 2H, CH_2-16), 2.62 – 2.37 (m, 3H, CH_2-12, C*H*H-11), 2.27 – 2.15 (m, 1H, CH*H*-11'), 1.48 (s, 18H, C(CH_3)$_3$-3, C(CH_3)$_3$-6), 1.45 (s, 9H, C(CH_3)$_3$-10). ^{13}C NMR (101 MHz, $CDCl_3$): δ = 170.3 (13), 169.5 (8), 155.7 (21), 152.4 (4, 1), 144.5 (14), 129.0 (19), 118.3 (15), 110.2 (18), 105.9 (20), 83.0 (9), 81.4 (5, 2), 58.5 (7), 55.4 (22), 48.5 (17), 32.7 (12), 28.1 (10, 6, 3), 25.1 (16), 24.6 (11). ESI-MS calcd for $C_{28}H_{42}N_2O_8$ (MH^+) 535.3, found 535.4.

*Nitration of **4** using Claycop.* To a solution of **4** (4.5 g, 8.46 mmol) in CCl_4 (35 mL) and Ac_2O (18 mL) was added Claycop 10/15 (5.41 g). The mixture was stirred for 2 h, after which the reaction was filtered over celite and the solid washed with CH_2Cl_2. The filtrate was evaporate in vacuo and the residue was dissolved in ethyl acetate (80 mL), washed with 1 M $NaHCO_3$ (50 mL), brine (50 mL), dried with $MgSO_4$, and concentrated in vacuo to give a crude mixture of 7-nitro and 5-nitro isomers of **5** and the mono-Boc decomposition product **6**. The mixture was purified by reverse-phase chromatography using a gradient of CH_3CN in H_2O containing 0.1% TFA, and fractions of **5** and **6** containing the major regioisomer (7-nitro) were isolated for characterization. Fractions of **5** contained a varying amount of compound **6** due to post-purification decomposition.

*4-Methoxy-7-nitroindolinyl N-α-(di-tert-butoxycarbonyl)-L-glutamic acid α-tert-butyl ester (**5**).* ^{1}H NMR (400 MHz, $CDCl_3$): δ = 7.73 (d, J = 9.0 Hz, 1H, Ar*H*-19), 6.63 (d, J = 9.1 Hz, 1H, Ar*H*-20), 4.77 (dd, 1H, C*H*-7), 4.22 (t, 2H, CH_2-17), 3.90 (s, 3H, CH_3-22), 3.06 (t, 2H, CH_2-16), 2.71 – 2.46 (m, 3H, C*H*H-11, CH_2-12), 2.23 – 2.13 (m, 1H, CH*H*-11'), 1.48 (s, 18H, C(CH_3)$_3$-3, C(CH_3)$_3$-6), 1.44 (s, 9H, C(CH_3)$_3$-10). ^{13}C NMR (101 MHz, $CDCl_3$): δ = 170.8 (13), 169.3 (8), 158.9 (21), 152.5 (4, 1), 136.8 (14), 135.4 (18), 125.5 (19), 122.9 (15), 106.3 (20), 83.4 (9), 81.7 (5, 2), 58.5 (7), 56.1 (22), 50.1 (17), 32.6 (12), 28.1 (10, 6, 3), 26.4 (16), 25.1 (11). ESI-MS calcd for $C_{28}H_{41}N_3O_{10}Na$ (M+Na) 602.3, found 602.4.

*4-Methoxy-7-nitroindolinyl N-α-(tert-butoxycarbonyl)-L-glutamic acid α-tert-butyl ester (**6**).* $[\alpha]_D^{20}$ = -16.9° (*c* 1.0, $CDCl_3$); ^{1}H NMR (400 MHz, $CDCl_3$): δ = 7.75 (d, J = 9.0 Hz, 1H, Ar*H*-17), 6.64 (d, J = 9.1 Hz, 1H, Ar*H*-18), 5.18 (d, 1H, N*H*-1), 4.27 – 4.12 (m, 3H, C*H*-2, CH_2-15), 3.91 (s, 3H, CH_3-20), 3.08 (t, 2H, CH_2-14), 2.67 – 2.46 (m, 2H, CH_2-10), 2.33 – 2.20 (m, 1H, C*H*H-9), 2.07 – 1.93 (m, 1H, CH*H*-9'), 1.46 (s, 9H, C(CH_3)$_3$-8), 1.44 (s, 9H, C(CH_3)$_3$-5). ^{13}C NMR (101 MHz, $CDCl_3$): δ = 171.5 (11), 170.9 (3), 158.9 (19), 155.9 (6), 136.6 (12), 135.4 (16), 125.5 (17), 122.9 (13), 106.4 (18), 82.5 (4), 80.1 (7), 56.1 (20), 53.8 (2), 50.1 (15), 32.0 (10), 28.4 (5), 28.2 (9), 28.1 (8), 26.4 (14). ESI-MS calcd for $C_{23}H_{33}N_3O_8$ (MH^+) 480.2, found 480.3.

*4-Methoxy-7-nitroindolinyl N-α-(9-fluorenylmethyloxycarbonyl)-L-glutamic acid (**7**).* Fractions of **5** and **6** from above were pooled (4.3 mmol) and dissolved in 1:1 TFA:CH_2Cl_2 (60 mL). After stirring for 7 h, the reaction mixture was concentrated to dryness, dissolved in H_2O (30 mL), and cooled to 0 °C. Potassium carbonate (1.19 g, 8.6 mmol) was added to the solution of amino acid and stirred for 10 mins. at 0 °C before addition of a solution of Fmoc-OSu (1.59 g, 4.7 mmol) in dioxane (30 mL). The reaction was allowed to warm to room temperature and was stirred overnight. After diluting the reaction mixture with H_2O (50 mL) and removing dioxane in vacuo, the aqueous portion was extracted with 2x25 mL Et_2O and acidified to pH 2 with 1 M HCl. The acidic mixture was extracted 2x75 mL with CH_2Cl_2, dried with $MgSO_4$, and concentrated in vacuo to yield 2.35 g of **7** (4.3 mmol, 51% from **4**) as a tan foam. $[\alpha]_D^{20}$ = -14.5° (*c* 1.0, $CDCl_3$); ^{1}H NMR (400 MHz, $CDCl_3$): δ = 7.77 – 7.67 (m, 3H, Ar*H*-12, Ar*H*-17, Ar*H*-27), 7.58 (t, J = 7.6 Hz, 2H, Ar*H*-10, Ar*H*-15), 7.37 (t, J = 7.4 Hz, 2H, Ar*H*-11, Ar*H*-16), 7.31 – 7.26 (m, 2H, Ar*H*-9, Ar*H*-14), 6.60 (d, 1H, Ar*H*-28), 5.92 (d, 1H, N*H*-1), 4.41 – 4.28 (m, 3H, C*H*-2, CH_2-5), 4.23 – 4.14 (m, 3H, C*H*-6, CH_2-25), 3.85 (s, 3H, CH_3-30), 3.05 (t, 2H, CH_2-24), 2.83 – 2.70 (m, 1H, C*H*H-20), 2.68 – 2.56 (m, 1H, CH*H*-20'), 2.42 – 2.29 (m, 1H, C*H*H-19), 2.21 – 2.08 (m, 1H, CH*H*-19'). ^{13}C NMR (101 MHz, $CDCl_3$): δ = 175.0 (3), 171.4 (21), 158.9 (29), 156.7 (4), 144.0 (18), 143.8 (7), 141.3 (8, 13), 136.3 (22), 135.3 (26), 127.8 (11, 16), 127.2

(9, 14), 125.5 (27), 125.4 (15), 125.3 (10), 123.1 (23), 120.0 (12, 17), 106.6 (28), 67.4 (5), 56.0 (30), 53.7 (2), 50.2 (25), 47.1 (6), 32.1 (20), 27.5 (19), 26.3 (24). ESI-MS calcd for $C_{29}H_{27}N_3O_8$ (MH^+) 546.2, found 546.3.

Circular Dichroism (CD)

CD spectra of peptide hydrogels were collected on an AVIV 410 spectropolarimeter (AVIV Biomedical Inc., NJ). For wavelength spectra of APC1 and APC2 in water, a 1 wt % solution of peptide was prepared by dissolving lyophilized peptide in water at 5 °C. The peptide solution was transferred to a 0.1 mm path length cylindrical cell and placed in the spectrometer sample holder equilibrated at 5 °C. For temperature-dependent folding of 1 wt % hydrogels, a 2 wt % peptide solution was first prepared by dissolving lyophilized peptide in water and chilling on ice. Then, an equal volume of chilled 100 mM BTP, 300 mM NaCl, pH 7.4 buffer was added, gently mixed, and quickly transferred to a 0.1 mm path length cylindrical cell and placed in the spectrometer sample holder equilibrated at 5 °C. The CD spectra were collected from 200-260 nm or 200-400 nm as a function of temperature at 5 degree increments from 5-80 °C with 10 min equilibration at each temperature. For UV photolysis of 1 wt% hydrogels, the solution was prepared in a manner identical to the folding studies and placed in the spectrometer at 25 °C or 37 °C for 30 minutes. The hydrogel within the cylindrical cell was irradiated for the specified time interval, followed by recording the mean residue ellipticity at 216 nm. For APC1, irradiation and spectra were obtained at 10 second intervals for the first 60 seconds, then at 1 minute intervals for a total of 5 minutes. For APC2, irradiation and spectra were obtained at 1 minute intervals for a total of 15 minutes. At the final time point, a wavelength spectrum from 200-400 nm of each peptide was obtained. Peptide concentration was determined by UV spectroscopy using $\varepsilon_{220nm} = 16448\ M^{-1}cm^{-1}$ for cAPC1 and cAPC2 and $\varepsilon_{220nm} = 31144\ M^{-1}cm^{-1}$ for APC1 and APC2. The mean residue ellipticity $[\theta]$ was calculated from $[\theta] = (\theta_{obs}/10lc)/r$, where θ_{obs} is the measured ellipticity in degrees, l is the path length in centimeters, c is the concentration in molar, and r is the number of residues in the sequence. Each CD spectra shown

is representative of three individual experiments, where each data point represents the average of 30 measurements, with a variance in ellipticity of 0.2 millidegrees at each wavelength.

Oscillatory Rheology and Atomic Force Microscopy

Rheology experiments were performed on an AR-G2 Rheometer (TA Instruments, DE) equipped with a 25 mm stainless steel parallel plate geometry using a 0.5 mm gap height. A 2 wt% peptide solution was prepared by dissolving lyophilized peptide in water and chilling on ice. An equal volume of chilled 100 mM BTP, 300 mM NaCl, pH 7.4 buffer was added and gently mixed, then immediately transferred to the rheometer plate equilibrated at 5 ^{o}C. In separate experiments, APC1 gels were prepared in syringe, or as a preformed slab, and incubated for 1 hour at 37 °C. Gels were then shear-thinned delivered, or transferred as an intact gel slab, to the rheometer plate, respectively. A temperature ramp from 5 ^{o}C to the desired temperature (25 °C or 37 °C) over 100 seconds was performed, followed by a 30-60 minute dynamic time sweep using an angular frequency of 6 rad/s and application of 0.2% strain to monitor the storage (G') and loss (G'') modulus of the hydrogel. The resulting hydrogel was further evaluated by performing a frequency sweep from 0.1 to 100 rad/s and a strain sweep at 6 rad/s from 0.1% to 1000% strain. Oil was placed around the sample and on the plate to prevent evaporation. Each time, frequency and strain sweep is representative of experiments performed in triplicate, with a variance in reported storage/loss moduli values of 0.041 Pa.

For shear-thinning and recovery experiments, a dynamic time sweep was performed to monitor hydrogel formation using an angular frequency of 6 rad/s and 0.2% strain over 15-30 minutes. This was followed by a 30 second time sweep using an angular frequency of 6 rad/s and 1000% strain to thin the gel. A time sweep was then performed at 0.2% strain to monitor the recovery of the storage modulus.

For UV photolysis experiments, the rheometer was fitted with an electrically-heated 25 mm stainless steel parallel plate upper geometry (EHP) and a UV-curing lower geometry. UV irradiation intensity was set at 100% power (~123 mW/cm^2). A 1 wt% hydrogel solution was prepared as described above and transferred to the rheometer plate with the EHP equilibrated at 25 °C or 37 ^{o}C. A dynamic time sweep (angular frequency = 6 rad/s, 0.2% strain) was performed to monitor the storage and loss modulus of the resulting hydrogel. Oil was placed around the sample and on the plate to prevent evaporation. Then, a shear-thinning-recovery experiment was performed by applying 1000% strain to the hydrogel for 30 seconds, followed by decreasing the applied strain to 0.2%, and then monitoring the recovery of the storage modulus as a function of time. UV photolysis of the hydrogel was performed by irradiating the sample for 10 minutes at 100% power and immediately monitoring the change in storage modulus as a function of time over a total of ~15 minutes.

For AFM studies, colloidal probe force-indentation experiments were conducted using an Asylum Research MFP-3D (Santa Barbara, CA) AFM in a fluid cell environment and performed on three individual samples. A gold colloid tipped cantilever probe (SQube, Bickenbach, Germany) with a nominal sphere radius of 3 μm was used for indentation; the cantilever spring constant was calibrated using the thermal fluctuation method[4] and found to be 1.40 ± 0.03 N/m. Force-indentation data was captured up to a maximum applied load of 25 nN and fit to the Hertz contact model to extract the elastic modulus. Reported moduli values represent the average of three independent samples, with ten individual measurements made per sample.

TEM

Micrographs of diluted hydrogel samples were obtained using a Hitachi H-7650 transmission electron microscope at a voltage of 80 kV. Hydrogels were prepared 3 hours before each TEM experiment was to occur. For each sample, 2 wt % peptide stock solutions in water were prepared and chilled on ice. To each solution an equal volume of chilled 100 mM BTP, 300 mM

NaCl, pH 7.4 was added to initiate gelation. After 3 hrs incubation, a small aliquot of the resulting 1 wt% gel was removed, diluted 40x with water and mixed well. 2 μL of the resulting diluted gel sample was placed onto a 200 mesh carbon coated copper grid and excess sample liquid was blotted away with filter paper. A solution of 1% uranyl acetate was then added to the grid as a negative stain to enhance contrast between fibrils and the background. Excess stain was blotted away and the grids were imaged immediately. Images shown are representative of three individual experiments, with variance that is inherent in the histogram analysis.

Animal Studies:

Hydrogel Injection and Anastomosis

A 2 wt% APC1 hydrogel was formed in a syringe by preparing a 4 wt% solution of lyophilized peptide in water and chilling on ice. An equal volume of chilled 100 mM BTP, 300 mM NaCl, pH 7.4 buffer was added and gently mixed, then immediately drawn up into a 1 mL disposable syringe. The syringe opening was capped and the syringe containing the 2 wt% solution was incubated at 25 ^{o}C for 1 hr. The mouse femoral artery was isolated and clamped prior to injection of the hydrogel into the divided vessel ends. The anastomosis was then performed according to the procedure described in the text, followed by irradiation of the vessel at 365 nm for 2 minutes using an OPTI-LUX 365 UV-A LED Flashlight (Spectroline, USA) at a distance of 5 mm above the surface of the vessel (~30 mW/cm^2). Two animal groups were employed, group 1 (anastomosis with gel) n= 16, and group 2 (anastomosis without gel) n=9. Animals were randomly distributed into each group without blinding or applied inclusion/exclusion criteria. The animal study was conducted in accordance with the Johns Hopkins University Animal Care and Use Committee Guidelines.

Histological Analysis

Mouse femoral arteries were harvested on days 0 and 7 post surgery. A 3-5 mm vessel segment containing the suture anastomosis site was obtained and fixed in 10% phosphate buffered

formalin for 24 hours. Tissue specimens were paraffin embedded under loop magnification to ensure proper orientation for cross sectional cutting. Sections at the location of the suture anastomosis defined as those sections containing nylon suture material were selected and stained with H&E, Masson Trichrome, and Elastic stains (e.g. VVG Verhoeff-Van Giessen). Histological samples were prepared from each group (anastomosis with gel, n= 3 and anastomosis without gel, n=3), with representative images shown below.

Spectral-Domain Optical Coherence Tomography (SD-OCT)

Spectral-Domain OCT was performed at various time points as described in the text. The spectrometer detector consisted of a line-scan camera (EM4, e2v, USA) with 12-bit depth and 2048 pixels. The light source was a superluminescent diode with an output power of 10 mW and an effective bandwidth of 105 nm centered at 845 nm. The system ran at a line rate of 70 kHz with an axial resolution of 3.0 micron in air and a transversal resolution of ~12 micron. The detectable range of the velocity of flowing target projected to the parallel direction of the scanning beam was $[-14.2;-0.294] \cup [0.294; 14.2]$ mm⁄s. For the images, 1000 A-scans were compiled to construct each B-scan image, and 250 B-scans were compiled to construct each C-scan image[5]. Blood flow speed analyses were performed on live mice that received femoral artery anastomosis with (n=3) and without APC1 gel (n=3) according to previously reported methodology.[6]

Perfusion Imaging

Micro CT and 3D reconstruction after APC1 hydrogel supported end-to-end anastomosis was performed by accessing the abdominal cavity of mice (n=5) through a midline incision to expose and cannulate the descending aorta at the level of the renal arteries using a soft intra-arterial catheter (Instech, Carotid Artery Catheter for Rats, #C19PU-RCA1301). Using heparinized saline (1:1000 Units) at a flow rate of about 5 mL/min, blood was gently flushed out of the circulation of the lower extremity through an incision made into the infra hepatic inferior vena

cava. After visible blanching of viscera and extremities the perfusion medium was changed to MicroFil, a solidifying silicone rubber (Flow Tech Inc.). MicroFil consists of a pigmented compound, diluent and curing agent mixed immediately prior to injection at the ratio 2 ml:5 ml:225 μL. Following injection the entire hind limb was imaged using high resolution Super Argus PET-μCT scanner (Sedecal). Scans were performed at 15-150 μm resolution isotropic voxels, 720 views, 350 ms integration time, 50 kVP, Scan time was 30-45 min. Images were processed using Amira (FEI) using standard volume rendering modules. Separate animals (n=2) receiving the same treatment were dissected to access the lower limb arterial tree for direct visualization of polymer perfusion after fixation.

For the Indocyanine Green experiment, animals (n=2) were positioned in the usual fashion. Harvest of the limb was performed as part of a tangential study. A transverse incision was made following the fold of the groin. Blunt dissection allowed exposure of the femoral nerve, artery, and vein. These were then isolated and divided after injection of a heparin solution. The remaining thigh muscle groups as well as the sciatic nerve were transected to expose the mid-portion of the femur. This completely separated the limb from a collateral blood supply. The isolated and divided femoral artery was then injected with ~1 μL of experimental hydrogel approximately 1 mm into the lumen of the vessel with a 33 gauge cannula under direct visualization. Two minutes after the injection, the ultraviolet light (OPTI-LUX 365 UV-A LED Flashlight, ~30 mW/cm^2) was applied approximately 5 mm from the surface of the vessel for 2 minutes. There was slight manual force exerted by a forceps instrument on the surface of the vessel to break up any large blocks of material. A 33 gauge cannula was then used to inject 100 μL of 2.5 mg/mL ICG solution (IC Green, Akorn Inc., Somerset, New Jersey). Simultaneous with injection of the contrast dye, laser imaging of the limb (SPY Elite, Novadaq, Toronto, Canada) was performed for 68 seconds. The sequence was extracted and recompiled using Matlab (Mathworks, Nattuck, Massachusetts).

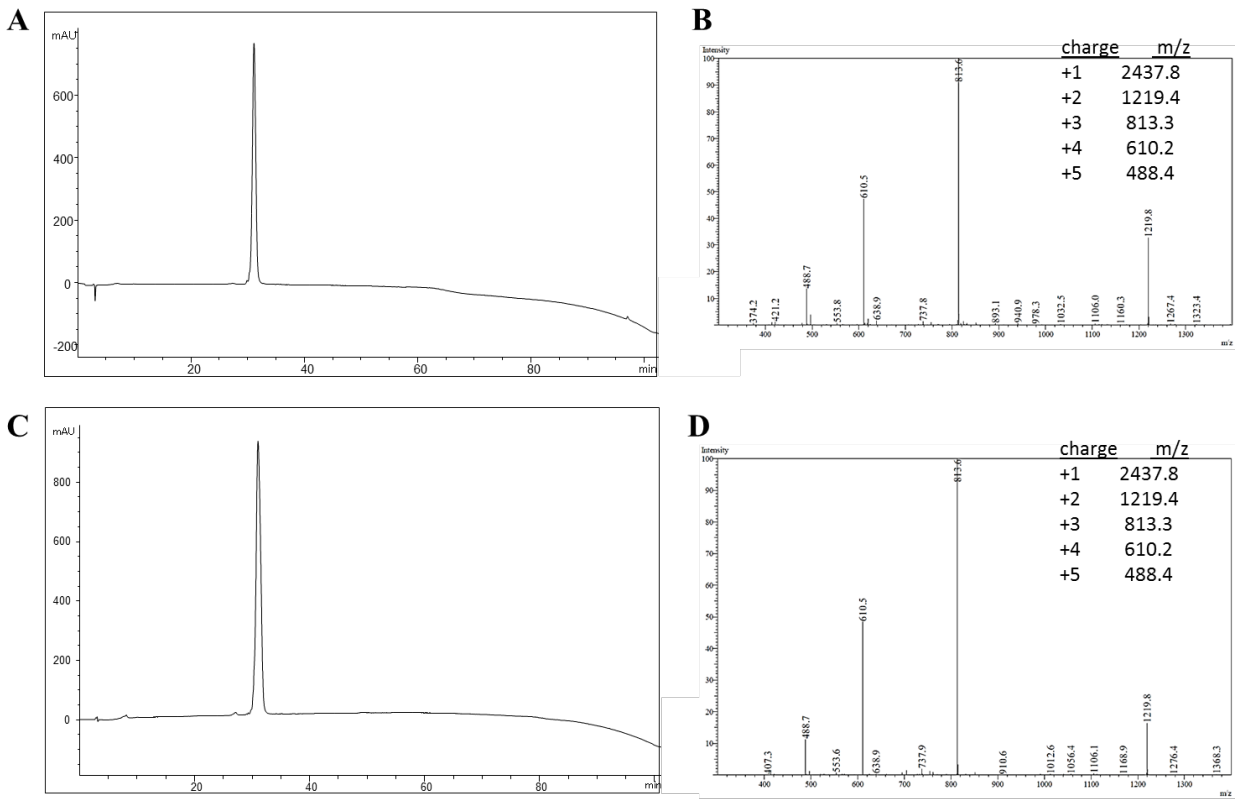

Supplementary Fig. 1. (A) HPLC of APC1. (B) Mass spectrum of APC1 with calculated m/z. (C) HPLC of APC2. (D) Mass spectrum of APC2 with calculated m/z.

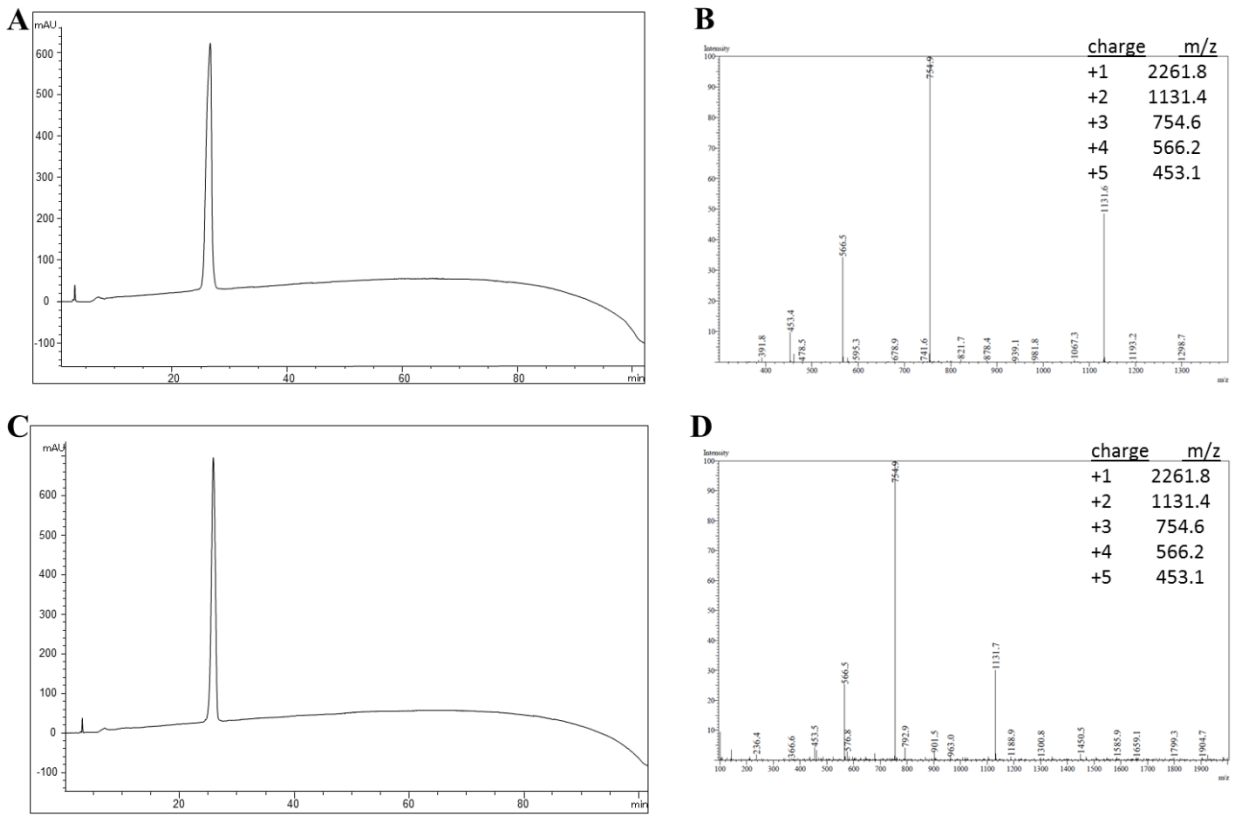

Supplementary Fig. 2. (A) HPLC of cAPC1. (B) Mass spectrum of cAPC1 with calculated m/z. (C) HPLC of cAPC2. (D) Mass spectrum of cAPC2 with calculated m/z.

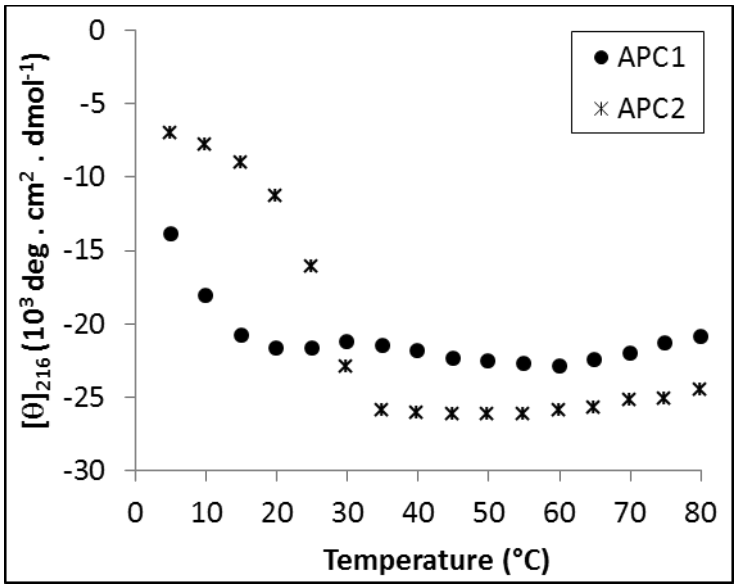

Supplementary Fig. 3. Temperature-dependent β-sheet formation for 1 wt% APC1 and APC2 hydrogels at pH 7.4, monitoring the mean residue elipticity [θ] at 216 nm.

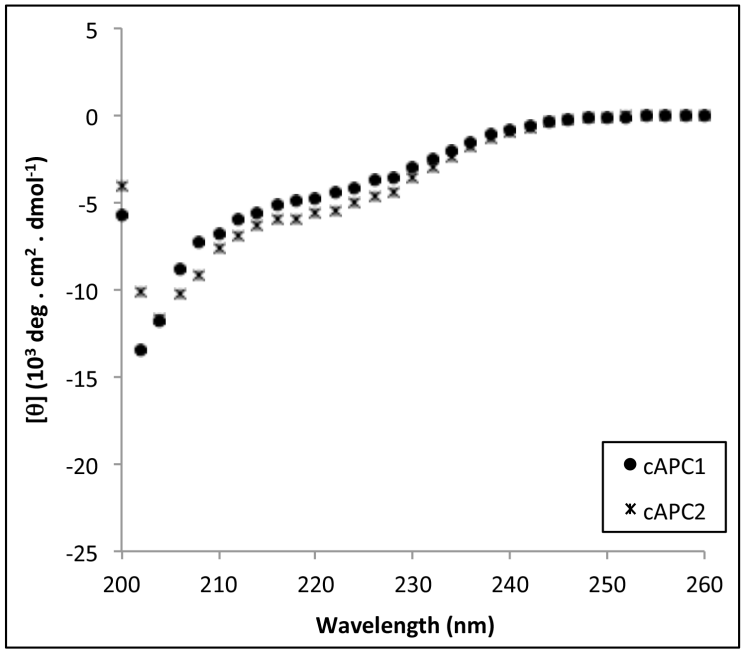

Supplementary Fig. 4. Spectra of 1 wt% controls, cAPC1 and cAPC2, at pH 7.4 (150 mM NaCl) and 25 and 37 °C, respectively.

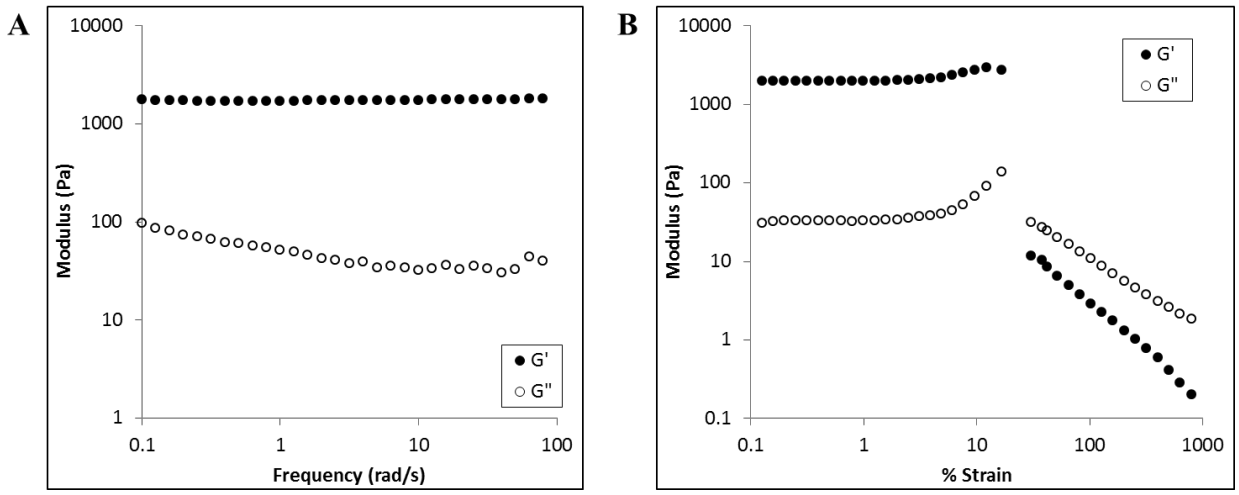

Supplementary Fig. 5. (A) Dynamic frequency sweep of 1 wt% APC1 (pH 7.4, 25 °C) at 0.2% strain. (B) Dynamic strain sweep of 1 wt% APC1 at a frequency of 6 rad/s.

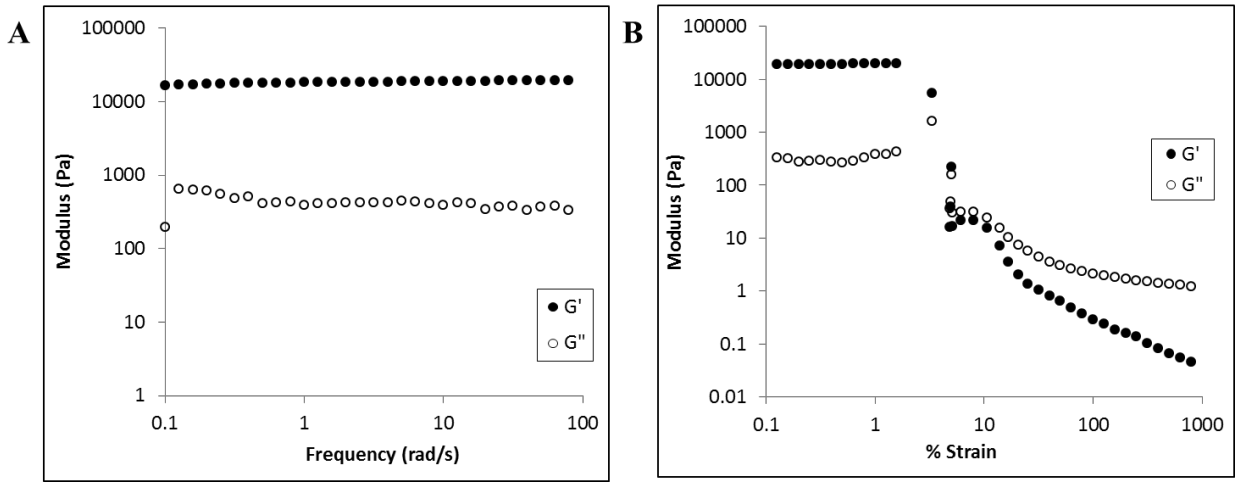

Supplementary Fig. 6. (A) Dynamic frequency sweep of 1 wt% APC2 (pH 7.4, 37 °C) at 0.2% strain. (B) Dynamic strain sweep of 1 wt% APC2 at a frequency of 6 rad/s.

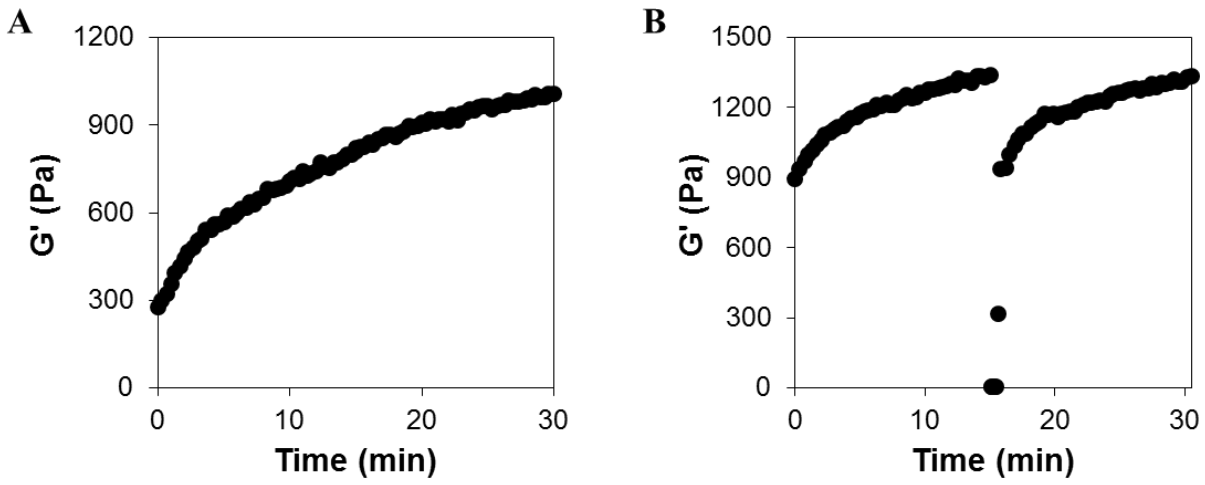

Supplementary Fig. 7. Rheological assessment of preformed APC1 gels to approximate material properties in a syringe. Dynamic time sweep of a pre-formed 1 wt% gel following its shear-thin delivery from a syringe directly onto the rheometer plate (A). Dynamic time sweep of a preformed gel slab that was transferred to the rheometer plate (B). Storage modulus (G') was monitored as a function of time at pH 7.4 and 37 °C ; frequency = 6 rad/s, 0.2% strain. For the preformed gel slabs (B), at 15 minutes 1000% strain was applied for 30 seconds to thin the material, after which the strain is decreased to 0.2% to allow material recovery.

Elastic Young's Modulus (E) [kPa]	Storage Modulus (G') [kPa]
10.6 ± 7.3	5.3 ± 3.7

Supplementary Table 1. Atomic force microscopy (AFM) measurements of preformed 1 wt% APC1 gels in PBS buffer. Force-indentation data was fit to the Hertz contact model to extract the elastic modulus (E). Storage modulus (G') was calculated using $G' = E/[2(1-\nu)]$, where the Poisson's ratio (ν) was approximated to be 0 for a highly porous material.

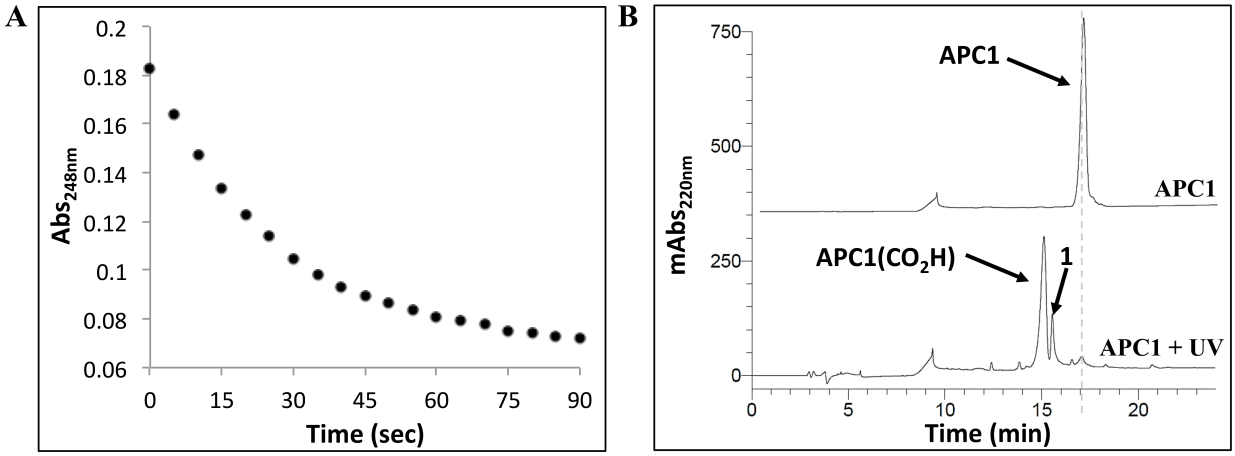

Supplementary Fig. 8. (A) UV absorbance of APC1's indoline cage as a function of time during photolysis. The absorbance of APC1 at 248 nm is followed as a function of time during irradiation. Absorbance at this wavelength is mainly due to the intact indoline cage. The observed rapid decrease in absorbance indicates that the indoline cage has undergone almost complete photolysis after 90 seconds of irradiation. Image shown represents averaged absorbance data for three independent experiments, with a variance in photometric accuracy of 0.005 AU. (B) RP-HPLC chromatograms of APC1. The top chromatogram shows intact APC1. The bottom chromatogram shows that after photolysis, uncaged peptide bearing a free glutamate side chain is produced along with the released photocage by-product **1**. Mass spectroscopy was used to confirm the identity of both species.

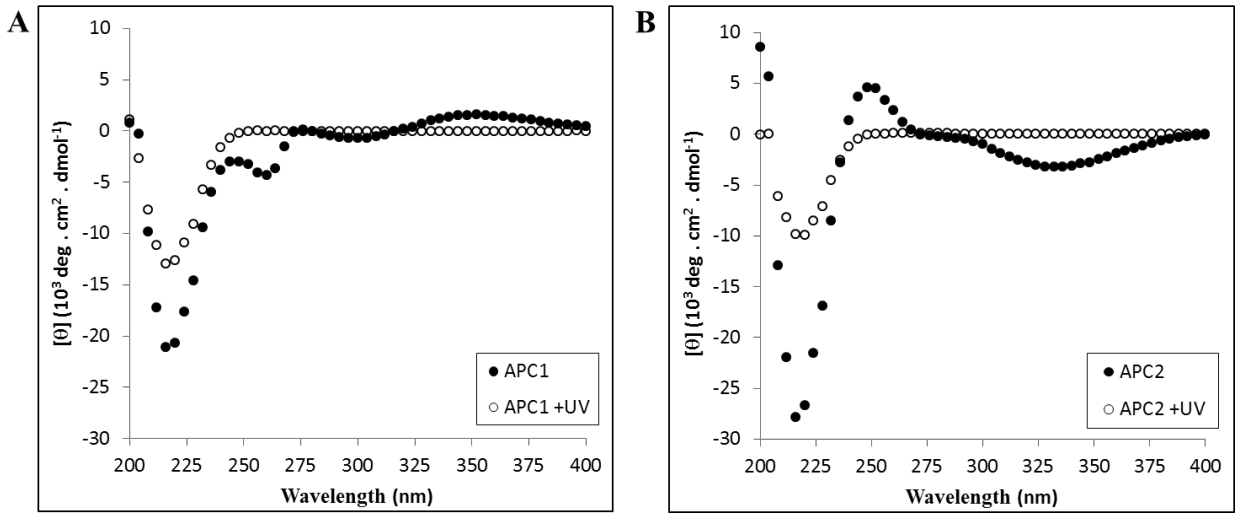

Supplementary Fig. 9. (A) Circular dichroism wavelength spectrum of 1 wt% APC1 (pH 7.4, 25 °C) before (●) and after (○) UV photolysis at 365 nm. (B) Circular dichroism wavelength spectrum of 1 wt% APC2 (pH 7.4, 37 °C) before (●) and after (○) UV photolysis at 365 nm.

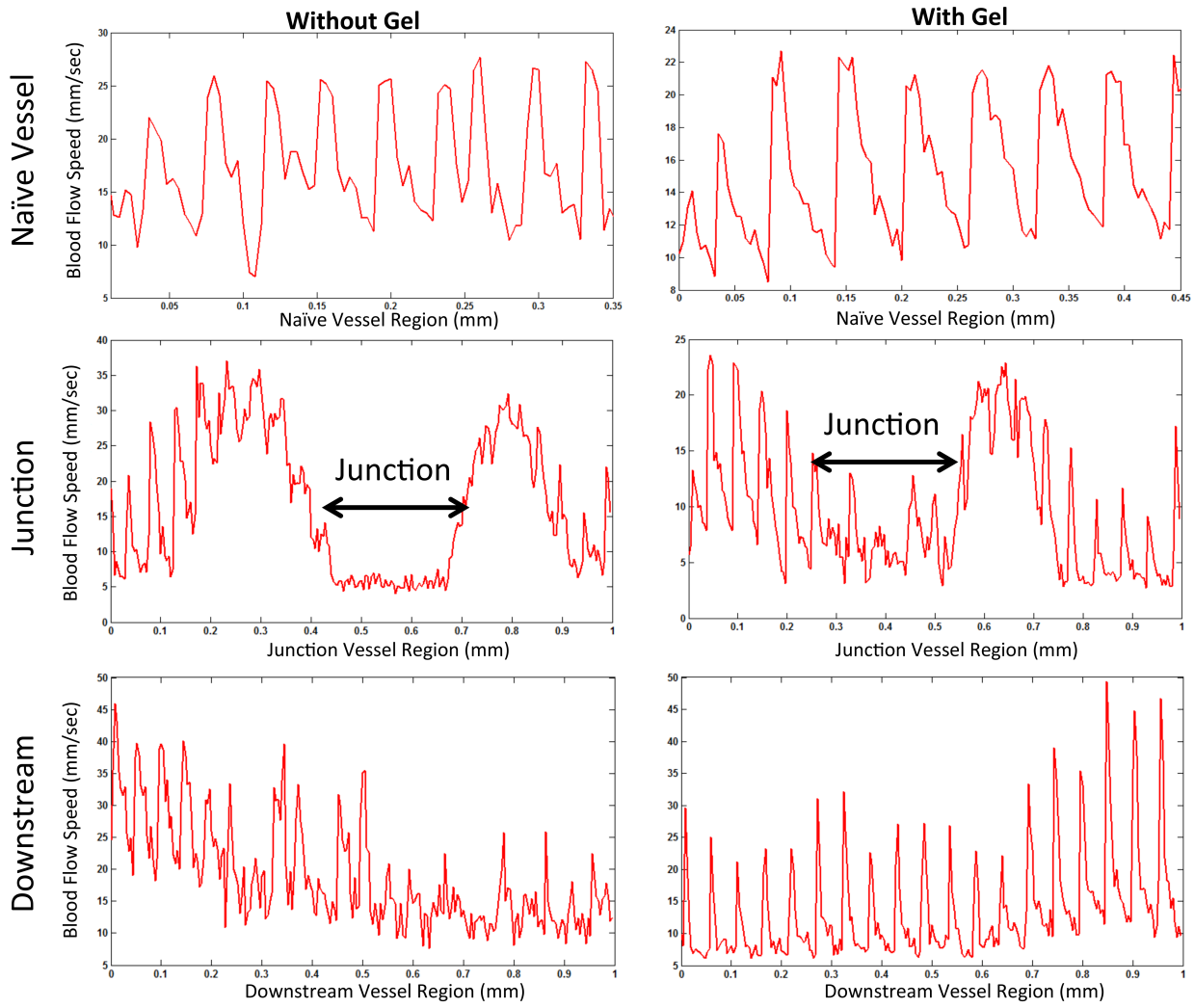

Supplementary Fig. 10. Phase-resolved Doppler optical coherence tomography was utilized to determine quantitative blood flow speed for mice receiving femoral artery anastomosis. Left column shows average artery blood flow speed measured in a vessel anastomosed without gel and right column shows vessel anastomosed with the APC1 gel. In each column, naïve vessels are compared to the junction (anastomosis) site, as well as the downstream vessel portion. The blood flow speed was calculated with a single Doppler angle deduced from the structure images and covers a range of 1 mm of the vessel. Normal flow speed was demonstrated for both conditions. Variations in blood flow speed between animals (e.g comparing the left and right columns) is a result of local Doppler angle nonuniformity.

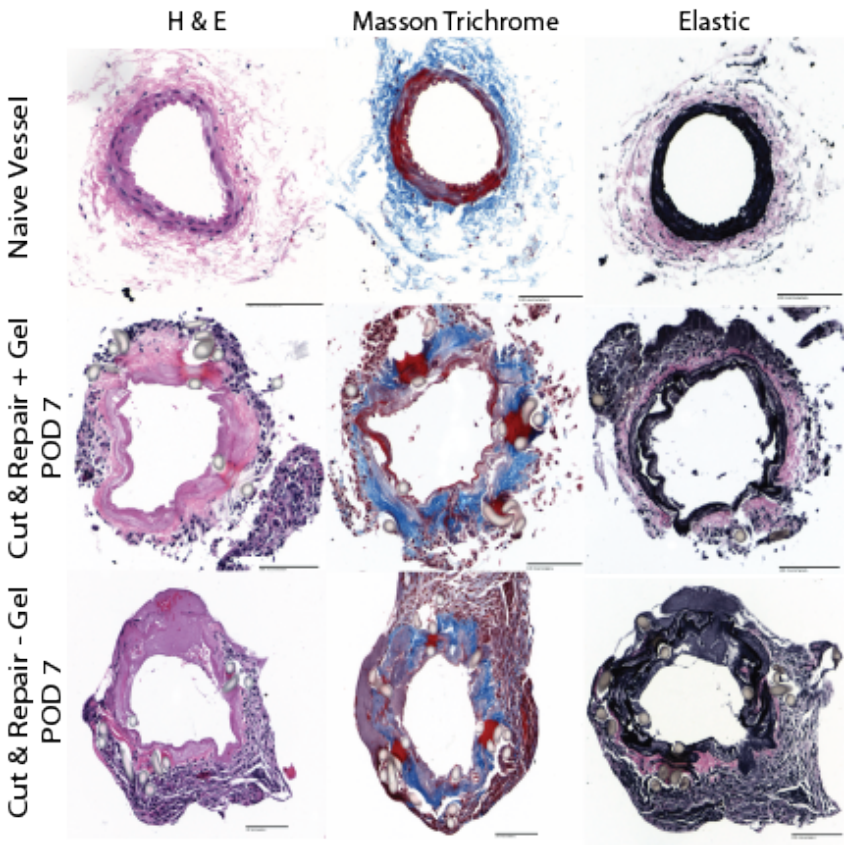

Supplementary Fig. 11. Histological images of anastomosed vessels 7 days post-surgery. Cross sections of mouse femoral arteries at the site of anastomosis (n=3, representative image of 1 animal). H&E, Masson Trichrome and Elastic stains were performed on naïve untreated control vessels, as well as samples obtained on post operative day 7 after anastomosis performed with and without the APC1 hydrogel. Compared to naïve vessels a peri-vascular inflammatory response can be appreciated in both anastomosis conditions as a result of the surgical tissue traumatization and the post operative physiologic healing process. However, the vascular lumen is free of remnants of the APC1 hydrogel comparable to the experiments without gel. No thrombus or endothelial inflammatory response is present indicating that the APC1 hydrogel has been completely dissolved. Scale bar = 100 micron.

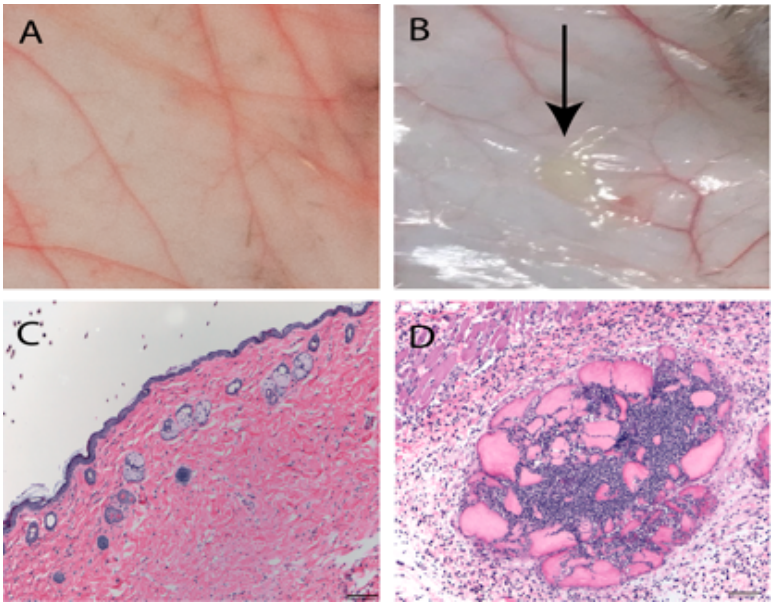

Supplementary Fig. 12. Histological evaluation of tissue surrounding subcutaneously implant site. Panel A and B show macroscopic images of the injection sites after either saline (A) or APC1 hydrogel (B, arrow head) application (50 µL) into the subcutaneous space of the lateral thoracic wall of mice (n=3, representative image of 1 animal) with no clinical signs of local inflammation. Panel C and D represent H&E stained histological cross sections of the skin and subcutaneous tissue from the local injection sites shown in A & B. While C shows no evidence of inflammatory cell infiltrates at the site of saline injection D shows APC1 hydrogel remnants with a surrounding of nucleated cells representative of a foreign body reaction. Ongoing degradation of the APC1 hydrogel can be appreciated by the fractioned gel components at 7 days post injection.

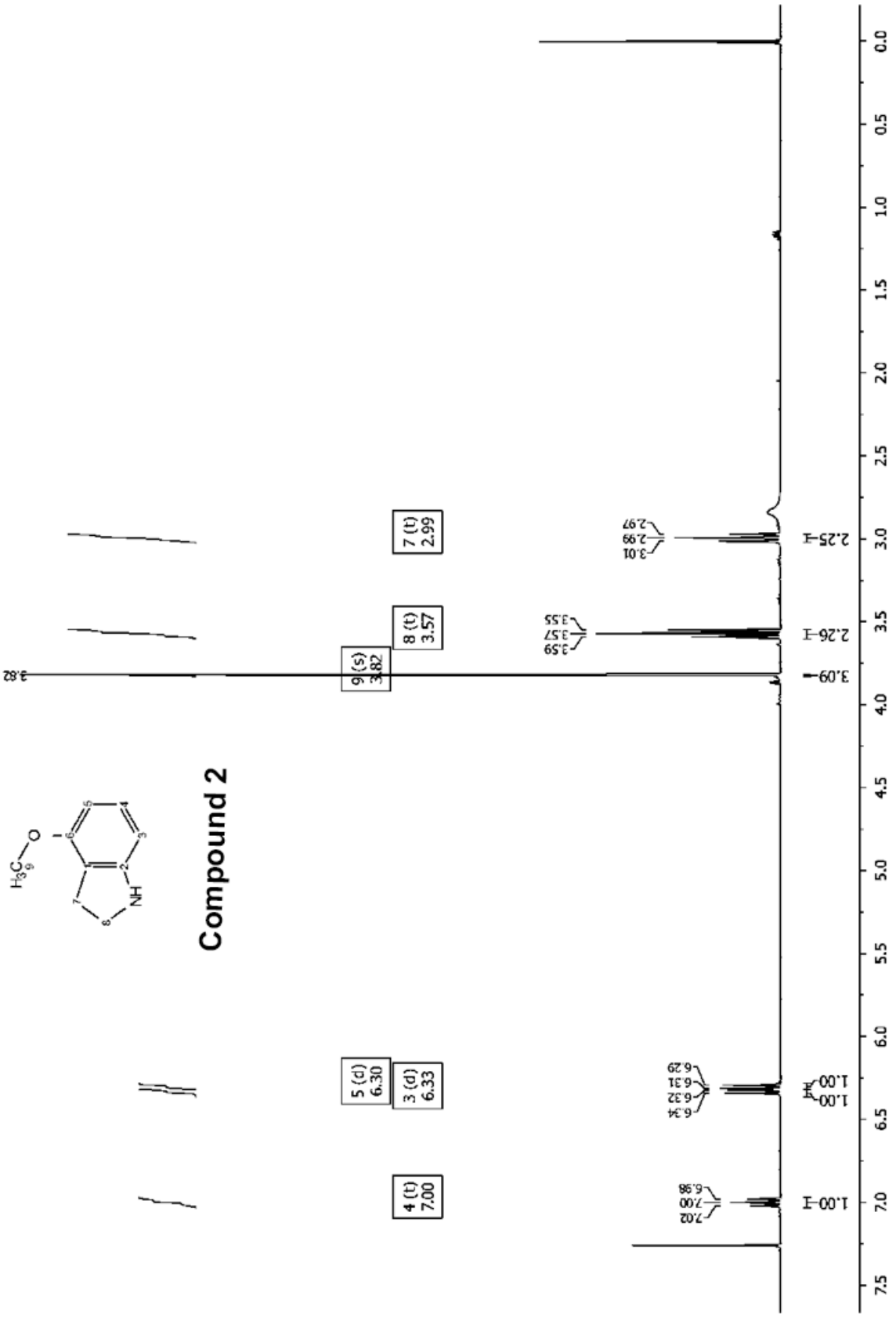
Compound 2
9 (s) 3.82
8 (t) 3.57
7 (t) 2.99
5 (d) 6.30
4 (t) 7.00
3 (d) 6.33
3.82
3.59
3.57
3.55
3.01
2.99
2.97
7.02
7.00
6.98
6.34
6.32
6.31
6.29
3.09
2.26
2.25
1.00
1.00
1.00
0.0
0.5
1.0
1.5
2.0
2.5
3.0
3.5
4.0
4.5
5.0
5.5
6.0
6.5
7.0
7.5

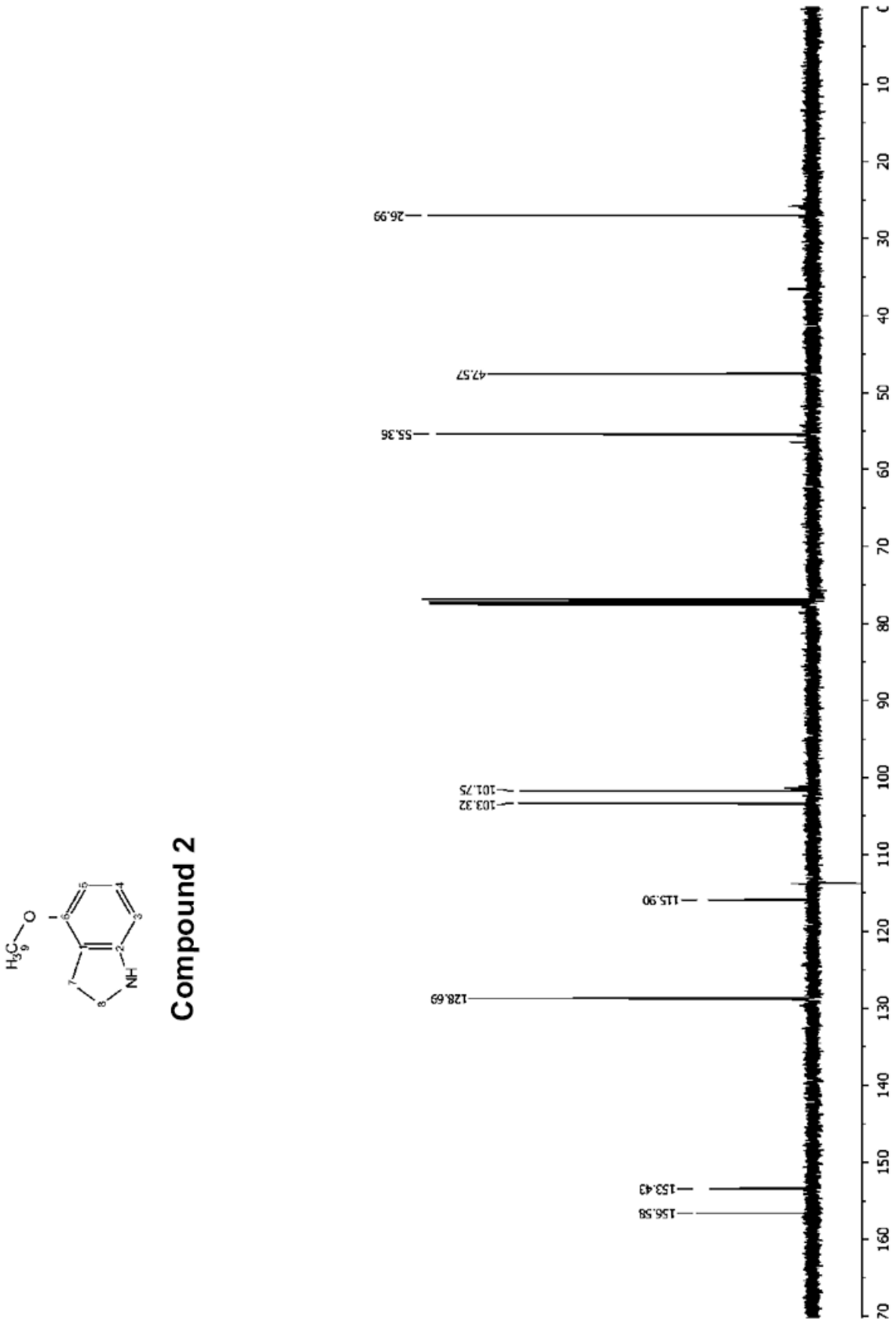
Compound 2
H3C
O
NH
26.99
47.57
55.36
101.75
103.32
115.90
128.69
153.43
156.58
10
20
30
40
50
60
70
80
90
100
110
120
130
140
150
160
170

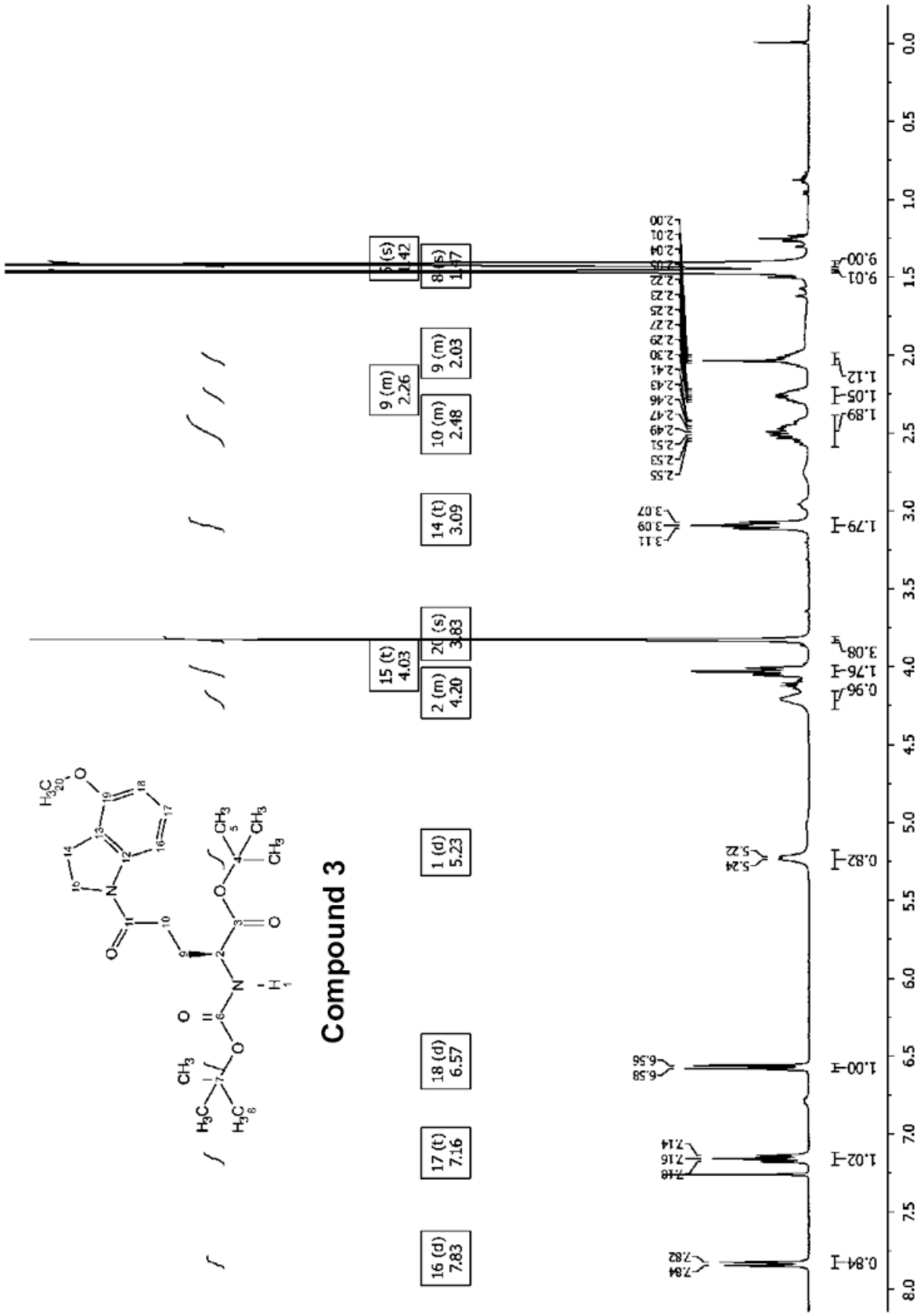
Compound 3
16 (d) 7.83
17 (t) 7.16
18 (d) 6.57
1 (d) 5.23
2 (m) 4.20
15 (t) 4.03
20 (s) 3.83
14 (t) 3.09
10 (m) 2.48
9 (m) 2.26
9 (m) 2.03
8 (s) 1.47
5 (s) 1.42
7.84
7.82
7.18
7.16
7.14
6.58
6.56
5.24
5.22
3.11
3.09
3.07
2.55
2.53
2.51
2.49
2.47
2.46
2.43
2.41
2.30
2.29
2.27
2.25
2.23
2.22
2.04
2.01
2.00
9.01
9.00
1.89
1.12
1.05
1.79
3.08
1.76
0.96
0.82
1.00
1.02
0.84

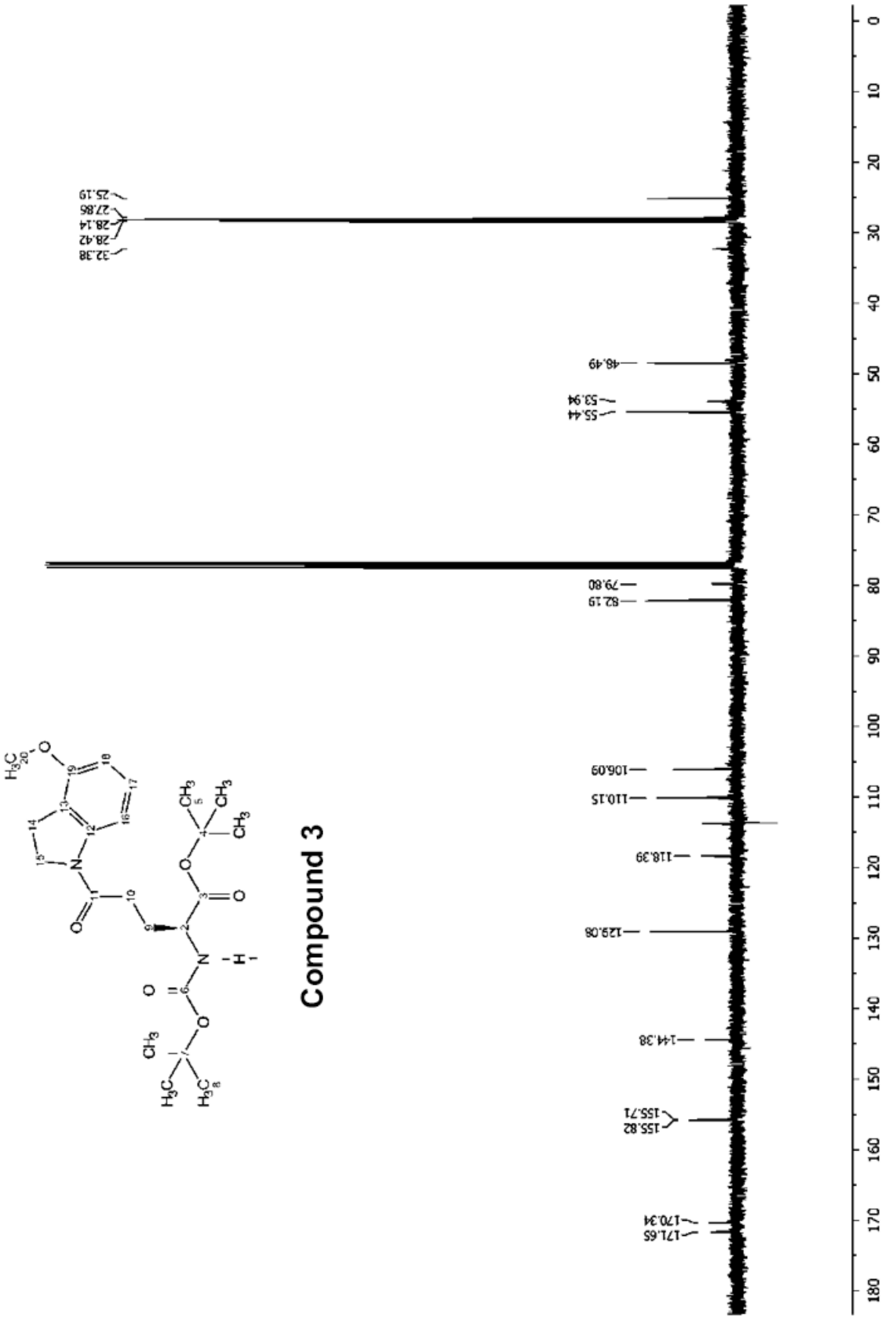
Compound 3
32.38
28.42
28.14
27.86
25.19
48.49
53.94
55.44
79.80
82.19
106.09
110.15
118.39
129.08
144.38
155.82
155.71
170.34
171.65

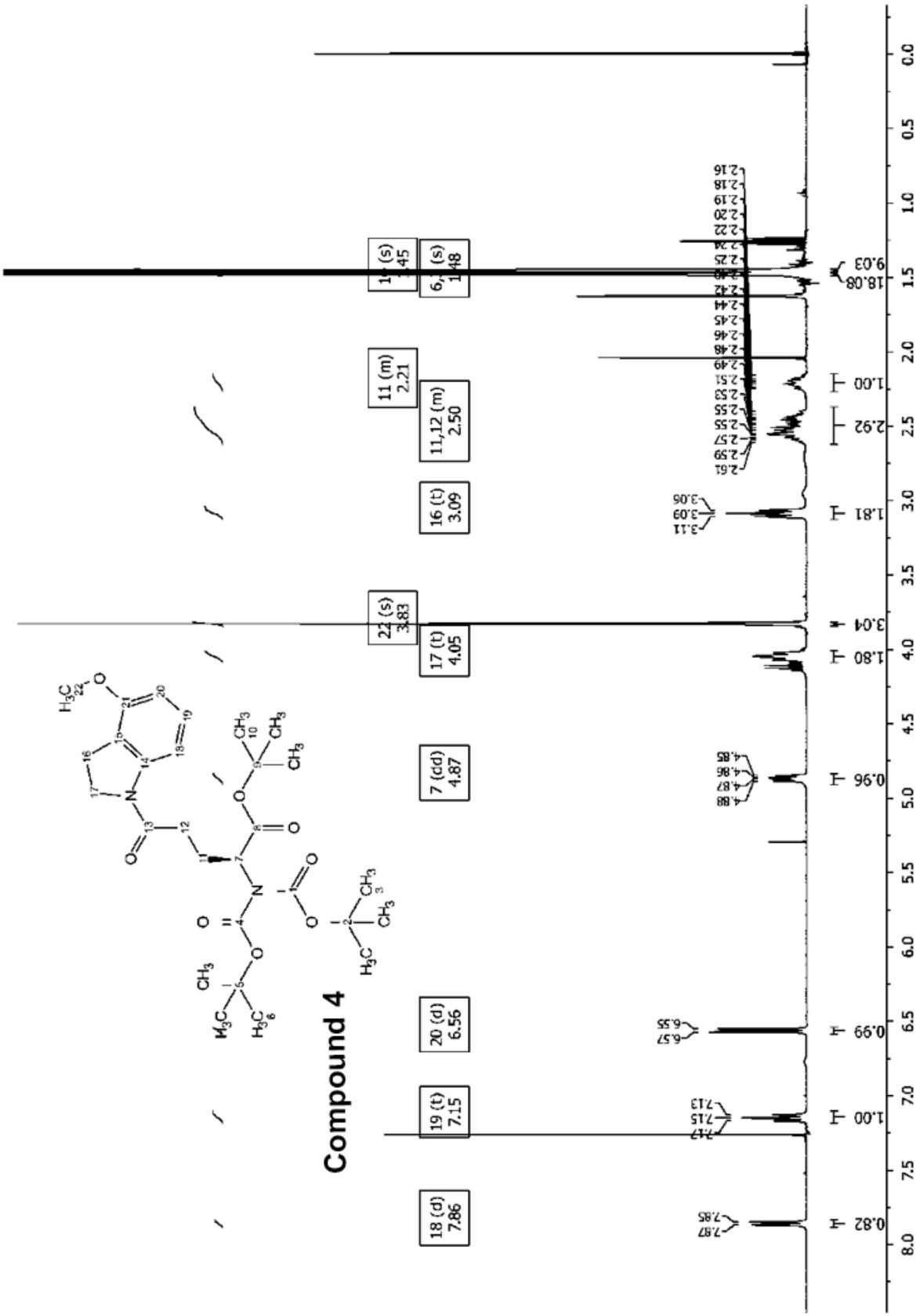
Compound 4
18 (d) 7.86
19 (t) 7.15
20 (d) 6.56
7 (dd) 4.87
17 (t) 4.05
22 (s) 3.83
16 (t) 3.09
11,12 (m) 2.50
11 (m) 2.21
6, (s) 1.48
0.82
1.00
0.99
0.96
1.80
3.04
1.81
1.00
2.92
18.08
9.03

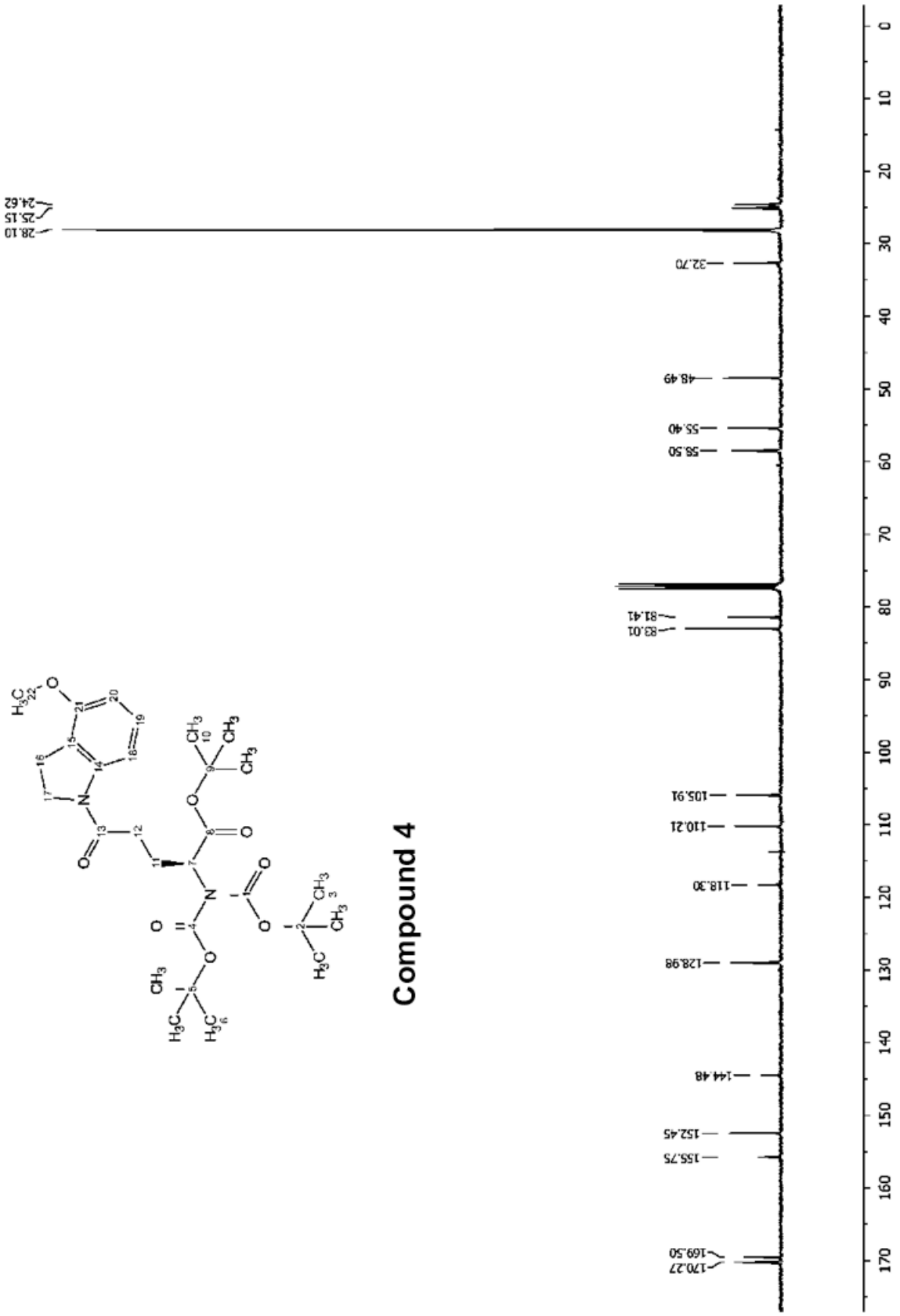
Compound 4
28.10
25.15
24.62
32.70
48.49
55.40
58.50
83.01
81.41
105.91
110.21
118.30
128.98
144.48
152.45
155.75
169.50
170.27
0
10
20
30
40
50
60
70
80
90
100
110
120
130
140
150
160
170

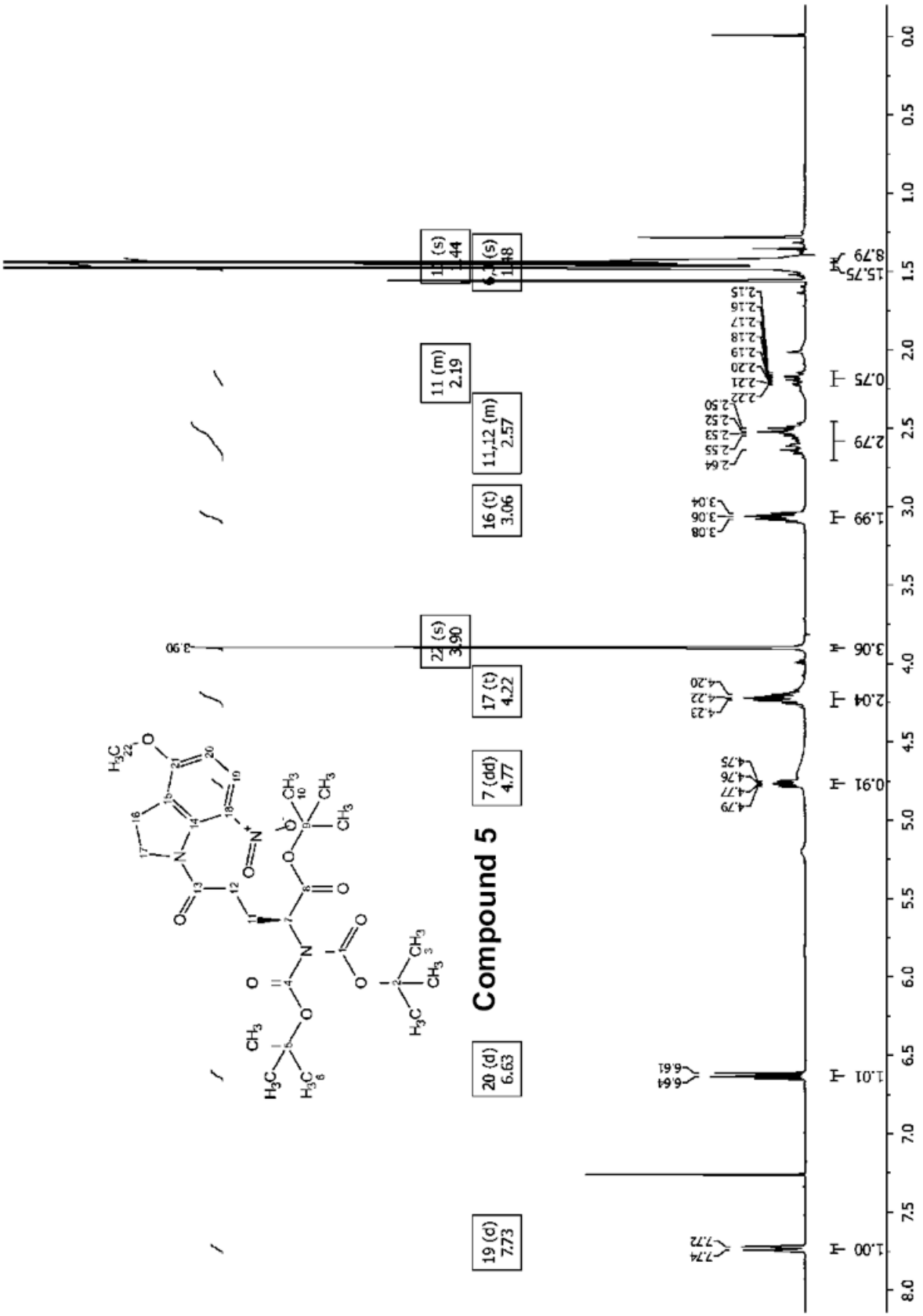
Compound 5
19 (d) 7.73
20 (d) 6.63
7 (dd) 4.77
17 (t) 4.22
21 (s) 3.90
16 (t) 3.06
11,12 (m) 2.57
11 (m) 2.19
18 (s) 1.38
15 (s) 1.44
7.74
7.72
6.64
6.61
4.79
4.77
4.76
4.75
4.23
4.22
4.20
3.08
3.06
3.04
2.64
2.55
2.53
2.52
2.50
2.22
2.21
2.20
2.19
2.18
2.17
2.16
2.15
8.79
15.75
1.00
1.01
0.91
2.04
3.06
1.99
2.79
0.75

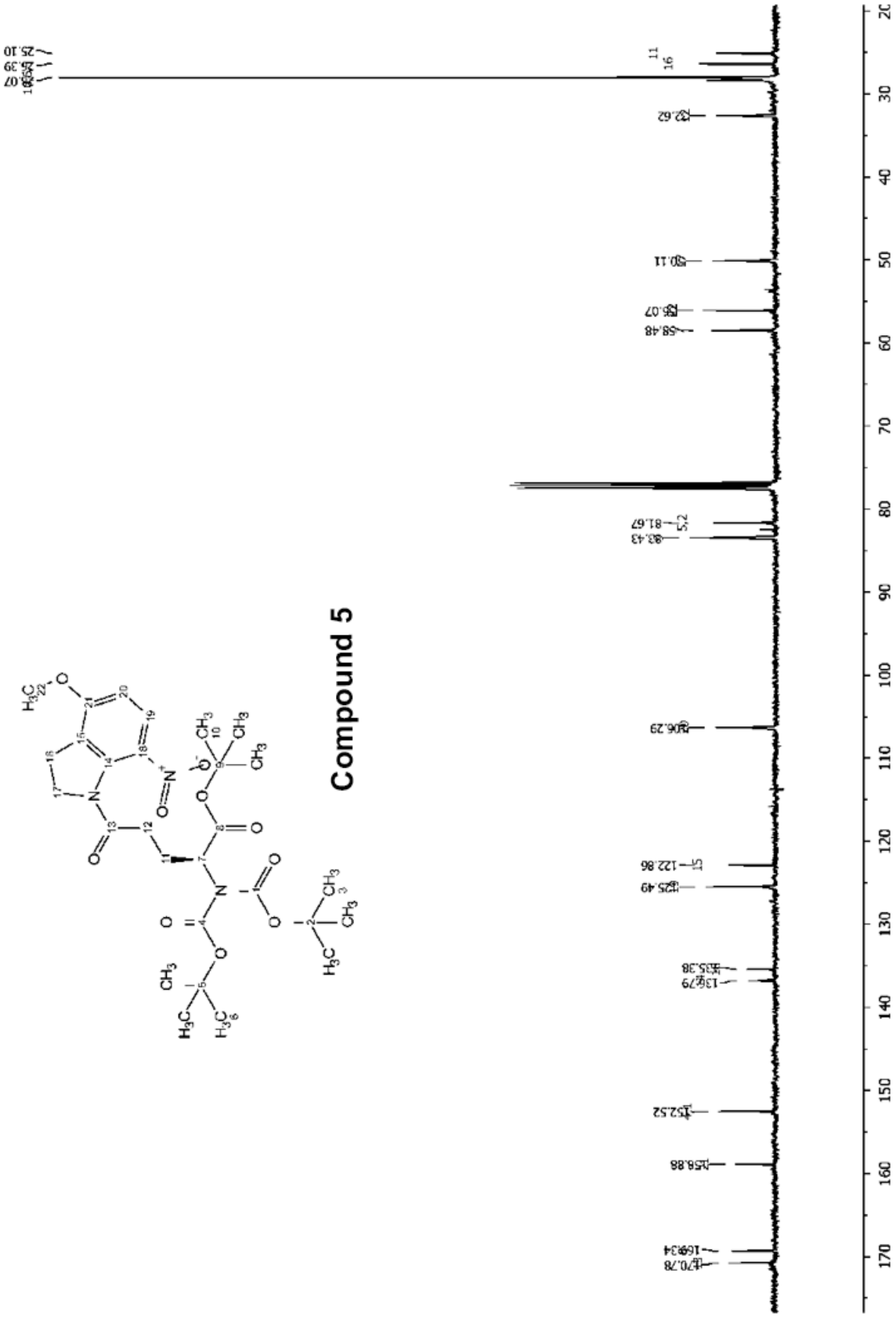
Compound 5

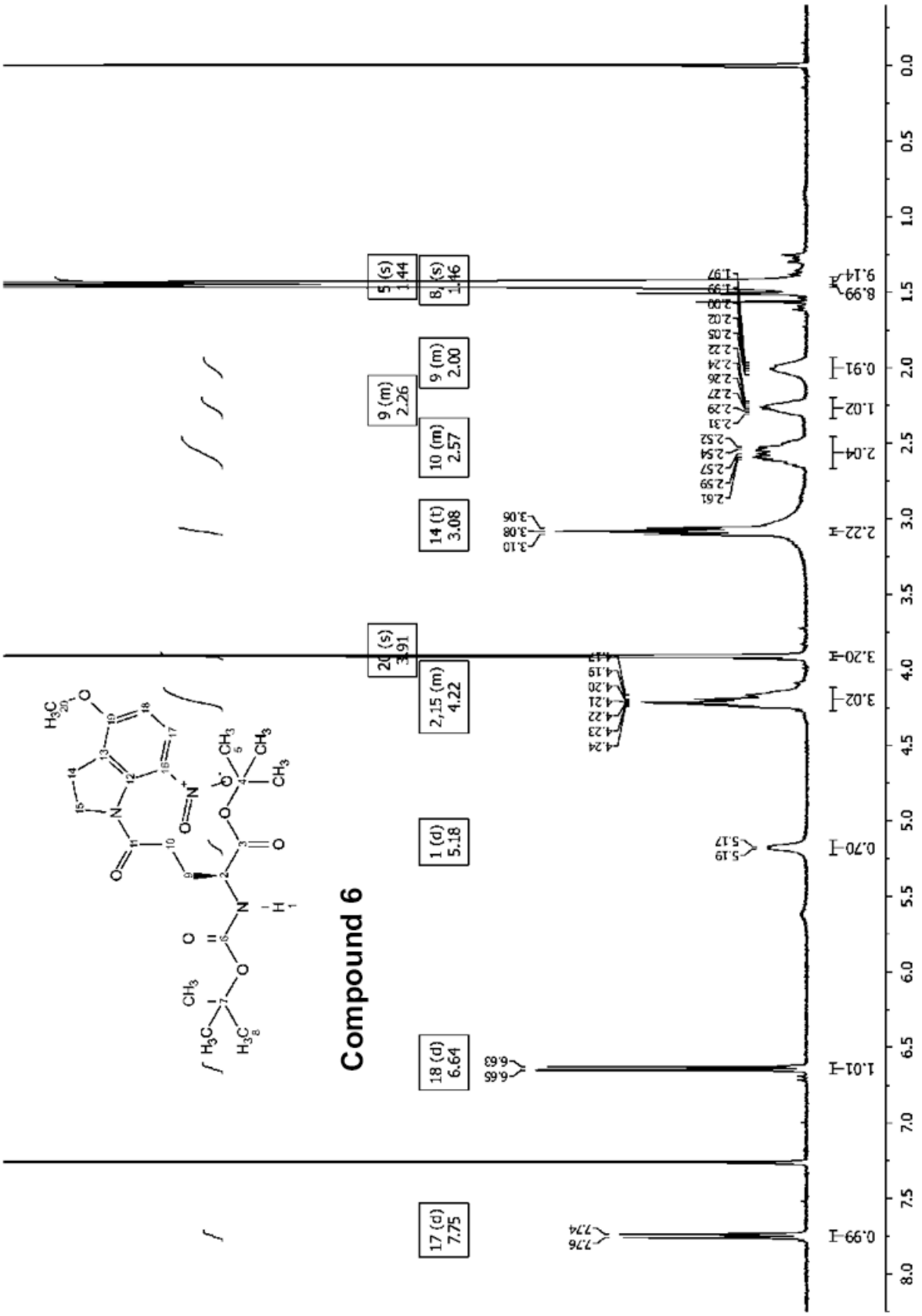
Compound 6
17 (d) 7.75
18 (d) 6.64
1 (d) 5.18
2,15 (m) 4.22
20 (s) 3.91
14 (t) 3.08
10 (m) 2.57
9 (m) 2.26
9 (m) 2.00
8 (s) 1.46
5 (s) 1.44
7.76
7.74
6.65
6.63
5.19
5.17
4.24
4.23
4.22
4.21
4.20
4.19
3.10
3.08
3.06
2.61
2.59
2.57
2.54
2.52
2.31
2.29
2.27
2.24
2.22
2.05
2.02
2.00
1.99
1.97
9.14
8.99
0.99
1.01
0.70
3.02
3.20
2.22
2.04
1.02
0.91

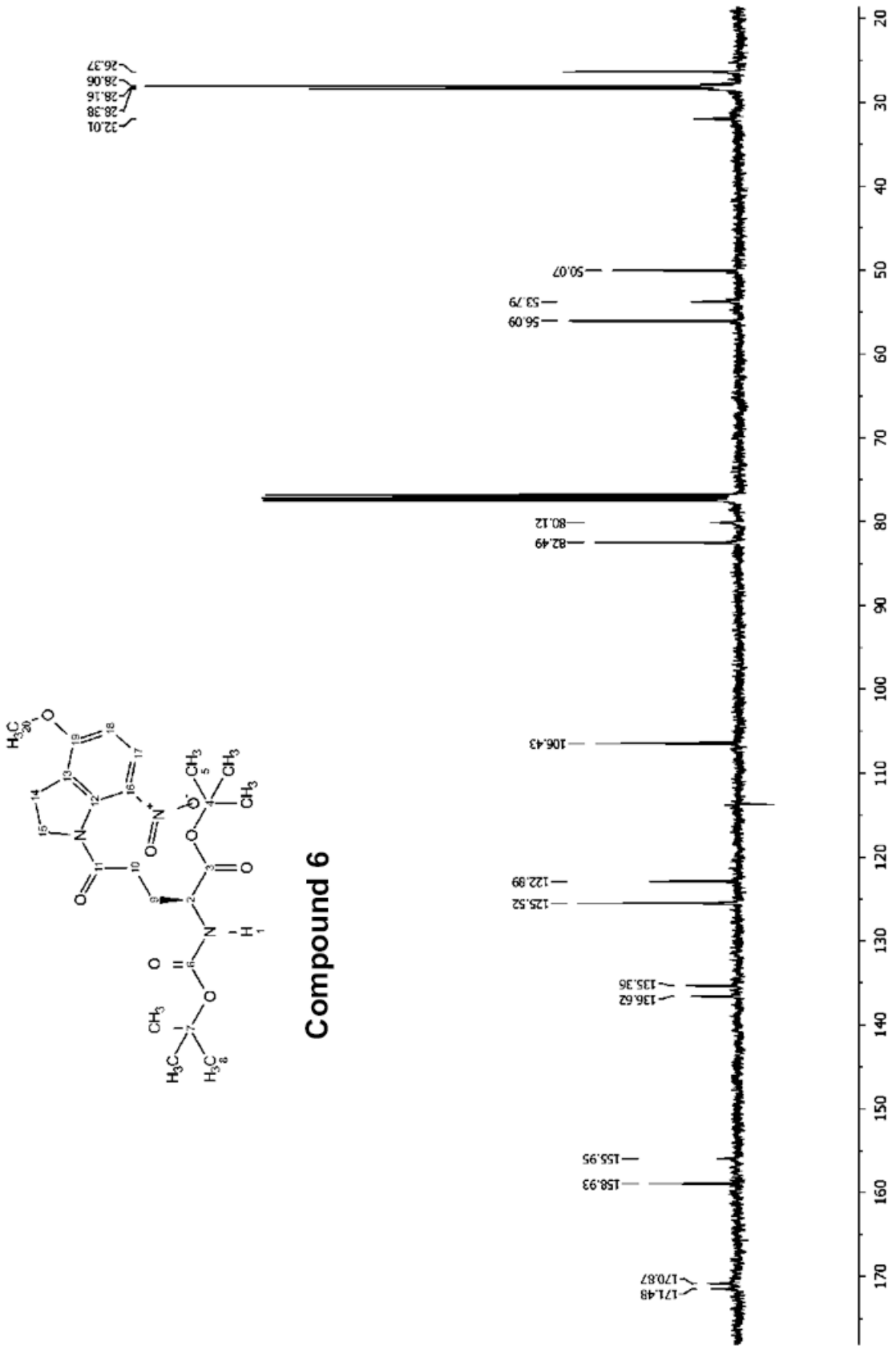
Compound 6
26.37
28.06
28.16
28.38
32.01
50.07
53.79
56.09
80.12
82.49
106.43
122.89
125.52
135.36
136.62
155.95
158.93
170.87
171.48
20
30
40
50
60
70
80
90
100
110
120
130
140
150
160
170

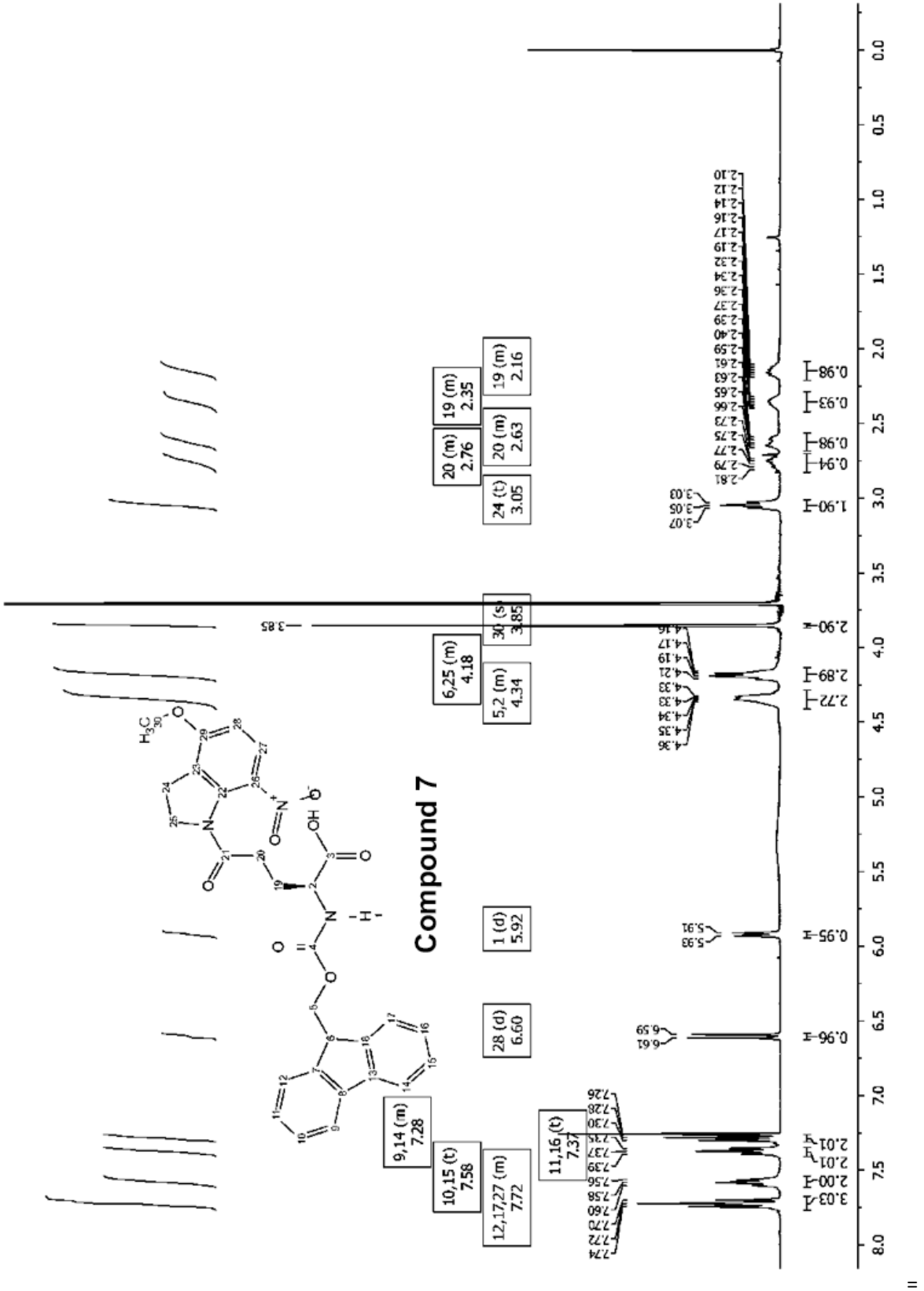
Compound 7
12,17,27 (m) 7.72
10,15 (t) 7.58
9,14 (m) 7.28
11,16 (t) 7.37
28 (d) 6.60
1 (d) 5.92
5,2 (m) 4.34
6,25 (m) 4.18
30 (s) 3.85
24 (t) 3.05
20 (m) 2.76
20 (m) 2.63
19 (m) 2.35
19 (m) 2.16

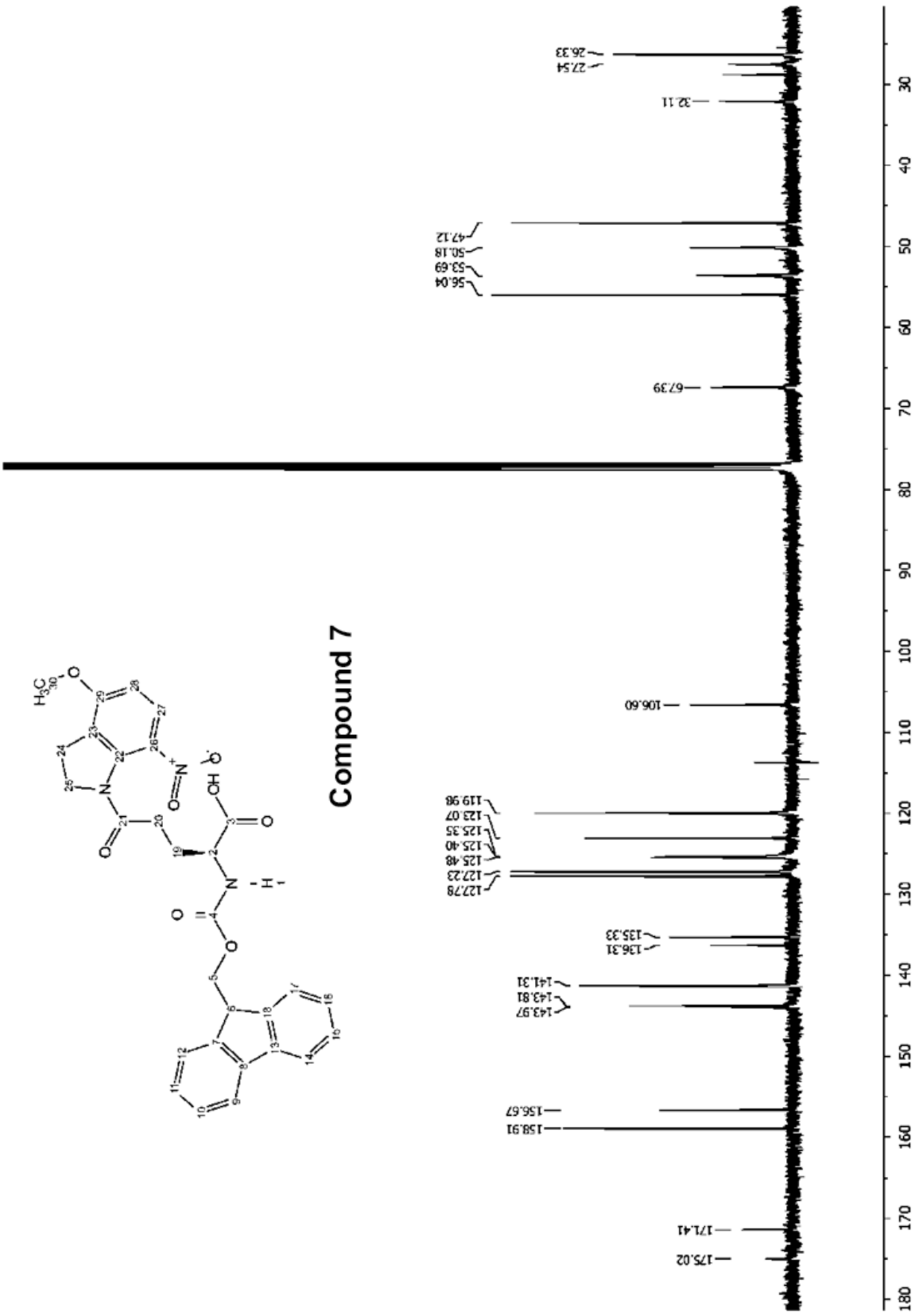
Compound 7
175.02
171.41
158.91
156.67
143.97
143.81
141.31
136.31
135.33
127.78
127.23
125.48
125.40
125.35
123.07
119.98
106.60
67.39
56.04
53.69
50.18
47.12
32.11
27.54
26.33

References

1. Papageorgiou, G.; Ogden, D.; Corrie, J. E. T. An antenna-sensitized nitroindoline precursor to enable photorelease of L-glutamate in high concentrations. *J. Org. Chem.* **69,** 7228 (2004).
2. Huang, Y. H.; Sinha, S. R.; Fedoryak, O. D.; Ellis-Davies, G. C. R.; Bergles, D. E. Synthesis and characterization of 4-methoxy-7-nitroindolinyl-D-aspartate, a caged compound for selective activation of glutamate transporters and N-methyl-D-aspartate receptors in brain tissue. *Biochemistry* **44,** 3316 (2005).
3. Laszlo, P.; Cornelis, A. Clay-supported cupric nitrite CLAYCOP, a user-friendly oxidizing and nitrating reagent. *Aldrichimica Acta* **21,** 97 (1988).
4. Butt, H. J.; Jaschke, M. Calculation of thermal noise in atomic-force microscopy. *Nanotechnol.* **6,** 1 (1995).
5. Huang, Y.; Ibrahim, Z.; Tong, D. D.; Zhu, S.; Mao, Q.; Pang, J.; Lee, W. P. A.; Brandacher, G.; Kang, J. U. Microvascular anastomosis guidance and evaluation using real-time three-dimensional Fourier-domain Doppler optical coherence tomography. *J. Biomed. Opt.* **18,** 11404 (2013).
6. Huang, Y.; Tong, D.; Zhu, S.; Wu, L.; Mao, Q.; Ibrahim, Z.; Lee, W. P. A.; Brandacher, G. Evaluation of Microvascular Anastomosis Using Real-Time, Ultra-High-Resolution, Fourier Domain Doppler Optical Coherence Tomography. *Plastic and Reconstructive Surgery* **135,** 711E (2015).